JPET Fast Forward. Published on May 12, 2017 as DOI: 10.1124/jpet.117.241976
This article has not been copyedited and formatted. The final version may differ from this version.

$S1P_1$-mediated anti-RAS cardioprotection: pivotal role of mast cell ALDH2

Alice Marino, Takuya Sakamoto, Pablo Robador, Kengo Tomita and Roberto Levi

Department of Pharmacology,

Weill Cornell Medicine,

New York, NY 10065

JPET Fast Forward. Published on May 12, 2017 as DOI: 10.1124/jpet.117.241976
This article has not been copyedited and formatted. The final version may differ from this version.

Running Title: $S1P_1R$/ALDH2-mediated anti-RAS cardioprotection

Corresponding author:

Roberto Levi, M.D., D.Sc., Department of Pharmacology,

Weill Cornell Medicine, 1300 York Avenue, New York, NY 10065

Phone 212-746-6223; rlevi@med.cornell.edu

Text pages: 55

Tables: 0

Figures: 9

References: 61

Abstract: 210 words

Introduction: 415 words

Discussion: 1386 words

Conclusions: 344 words

List of non-standard abbreviations:

ALDH2, aldehyde dehydrogenase type-2; **ALDH2*2**, a knock-in mouse model, in which ALDH2 enzymatic activity is radically reduced; **Ang I**, angiotensin I; **BMMC**, murine bone marrow-derived mast cells; **β-HEX**, β-hexosaminidase; **εV_{1-2}**, a selective PKCε inhibitor; **GTN**, glyceryl trinitrate, an ALH2 inactivator**; HMC-1**, a human mastocytoma cell line; **4-HNE**, 4-hydroxynonenal; **IPC**, ischemic preconditioning; **I/R**, ischemia/reperfusion; **MC**, mast cells; **NE**, norepinephrine; **PKCε**, Protein Kinase C subtype-ε; **PMA,** phorbol ester myristate acetate; **RAS**, renin-angiotensin system; **SEW287**, a selective $S1P_1R$ agonist; **S1P**, sphingosine-1-phosphate; **$S1P_1R$**, $S1P_1$ receptors; **TTC**, 2,3,5-Triphenyltetrazolium chloride; **VT/VF**, ventricular tachycardia/ventricular fibrillation; **WT**, wild-type C57BL/6J mice; **W146**, a selective $S1P_1R$ antagonist.

Recommended section assignment: Cardiovascular Pharmacology

JPET Fast Forward. Published on May 12, 2017 as DOI: 10.1124/jpet.117.241976
This article has not been copyedited and formatted. The final version may differ from this version.

Abstract

In the ischemic-reperfused (I/R) heart, renin-containing mast cells (MC) release enzymatically active renin, activating a local renin-angiotensin system (RAS), causing excessive norepinephrine release and arrhythmic dysfunction. Activation of G_i-receptors on MC, and/or ischemic preconditioning (IPC), prevent renin release, thus providing anti-RAS cardioprotection. We questioned whether sphingosine-1-phosphate (S1P), a sphingolipid produced in the I/R heart, might afford anti-RAS cardioprotection by activating G_i-coupled $S1P_1$ receptors ($S1P_1R$) on MC. We report that activation of G_i-coupled $S1P_1R$ in cardiac MC confers IPC-like anti-RAS cardioprotection due to $S1P_1R$-mediated inhibition of I/R-induced cardiac MC degranulation and renin release. This results from an initial translocation of protein kinase C subtype-ε **(**PKC_ε) and subsequent activation of aldehyde dehydrogenase type-2 (ALDH2), culminating in the elimination of the MC-degranulating effects of acetaldehyde and other toxic species produced during I/R. Inhibition of toxic aldehydes-induced MC-renin release prevents local RAS activation, reduces infarct size and alleviates arrhythmias. Notably, these cardioprotective effects are lacking in hearts and MC from gene-targeted knock-in mice (ALDH2*2) in which ALDH2 enzymatic activity is maximally reduced. Thus, ALDH2 appears to play a pivotal role in this protective process. Our findings suggest that MC $S1P_1R$ may represent a new pharmacologic and therapeutic target for the direct alleviation of RAS-induced cardiac dysfunctions, including ischemic heart disease and congestive heart failure.

JPET Fast Forward. Published on May 12, 2017 as DOI: 10.1124/jpet.117.241976
This article has not been copyedited and formatted. The final version may differ from this version.

Introduction

Excessive release of norepinephrine (NE) from cardiac sympathetic nerves during ischemia/reperfusion (I/R) is a cause of life-threatening arrhythmias (Airaksinen, 1999; Chen et al., 2001; Selwyn and Braunwald, 2001; Tan and Verrier, 2013). In previous studies we demonstrated that in the I/R heart, renin-containing mast cells (MC) release enzymatically active renin, activating a local renin-angiotensin system (RAS), which culminates in angiotensin-induced NE release from sympathetic nerves and severe arrhythmic dysfunction (Silver et al., 2004; Mackins et al., 2006). We reported that activation of G_i-coupled receptors, such as adenosine A_3 and histamine H_4, present on the MC surface, prevents MC degranulation and renin release in the I/R heart, thus attenuating angiotensin-induced NE release from sympathetic nerves and alleviating ventricular arrhythmias (Koda et al., 2010; Aldi et al., 2014b). Ischemic preconditioning (IPC) mimics this process via a G_i-mediated translocation/activation of MC PKCε, followed by phosphorylation/activation of mitochondrial aldehyde dehydrogenase type-2 (ALDH2) (Koda et al., 2010; Aldi et al., 2014b). PKCε translocates from cytosol to mitochondrial membrane and phosphorylates ALDH2 on three phosphorylation sites, threonine 185 (T185), serine 279 (S279) and threonine 412 (T412), resulting in increased catalytic activity of ALDH2 (Chen et al., 2008). By eliminating toxic aldehydes formed in I/R, and thus preventing MC degranulation and renin release, ALDH2 plays a pivotal anti-RAS cardioprotective role (Koda et al., 2010; Aldi et al., 2014b).

The sphingolipid sphingosine-1-phosphate (S1P) is formed in the ischemic heart, and S1P is thought to be cardioprotective and to mimic IPC via a PKCε-dependent step (Gray et al., 1997; Jin et al., 2004; Vessey et al., 2009). Accordingly, we questioned whether S1P might also afford anti-RAS cardioprotection by activating

G_i-coupled $S1P_1$ receptors ($S1P_1R$) on MC, and by PKCε-dependent ALDH2 phosphorylation (Chen et al., 2008).

We questioned whether the stimulation of $S1P_1R$ in both cavian and murine hearts mimics the anti-RAS effects of IPC by activating PKCε and ALDH2 in MC and thus, by inhibiting toxic aldehyde-induced MC-renin release. We also investigated whether this process is lacking in hearts and MC from gene-targeted knock-in mice (ALDH2*2) (Zambelli et al., 2014) in which ALDH2 enzymatic activity is maximally reduced, due to a structural point mutation at amino acid position 487 of ALDH2 (a lysine residue replaces a glutamate)(Xiao et al., 1996). We took advantage of the homozygous variant of ALDH2*2 knock-in mice, to probe whether the activation of G_i-coupled $S1P_1R$ in cardiac MC confers anti-RAS cardioprotection through a PKCε-dependent ALDH2 phosphorylation, prevention of toxic aldehydes-induced MC-renin release, inhibition of local RAS activation and ultimate anti-arrhythmic effects.

JPET Fast Forward. Published on May 12, 2017 as DOI: 10.1124/jpet.117.241976
This article has not been copyedited and formatted. The final version may differ from this version.

Materials and Methods

I/R in Guinea pig hearts

Guinea pigs (male Hartley, 300-350 g; Charles River Laboratories, Kingston, NY) were kept in the animal care facility under controlled temperature, humidity and light/dark cycle, with food and water ad libitum. The animals were anesthetized with CO_2 and euthanized by stunning while under general anesthesia. Hearts were rapidly isolated and perfused at constant pressure (55 cm H_2O) with oxygenated Ringer's solution (composition, mM: NaCl 154, KCl 5.61, $CaCl_2$ 2.16, $NaHCO_3$ 5.95 and dextrose 5.55) at 37°C in a Langendorff apparatus (Radnoti Glass Technology Inc., Monrovia, CA). After equilibration, all hearts were subjected to 20-min global ischemia, induced by complete cessation of coronary perfusion, followed by 30-min reperfusion (I/R). For IPC, hearts were subjected to 2 × 5-min cycles of ischemia, each followed by 5-min reperfusion. For the pharmacologic prevention of IPC, $S1P_1R$ antagonist was perfused for 20 min before and during IPC, and then washed out for 15 min before I/R. For pharmacologic preconditioning, $S1P_1R$ agonist (SEW2871, 1 μM) was perfused for 2 × 5-min cycles and then washed out for 5 min before I/R. For prevention of pharmacologic preconditioning, antagonists (W146 1 μM and PKCε inhibitor εV1-2 1 μM were perfused for 20 min, while the ALDH2 inhibitor GTN 2μM was perfused for 30 min) before and during pharmacologic preconditioning and then washed out for 15 min before I/R. Coronary flow was measured every 2 min; samples were assayed for renin and NE. Two needle electrodes were attached to the surface of the right atrium and left ventricular apex for ECG, which was recorded online (sample frequency of 1 kHz) and analyzed using Powerlab/8SP (ADInstruments, Colorado Springs, CO). Onset and duration of reperfusion arrhythmias were recorded and quantified according to the Lambeth Conventions (Walker et al., 1988; Curtis et al., 2013).

JPET Fast Forward. Published on May 12, 2017 as DOI: 10.1124/jpet.117.241976
This article has not been copyedited and formatted. The final version may differ from this version.

I/R in Mouse hearts

Hearts were isolated from male C57BL/6 wild-type (WT) and ALDH2*2 mice and perfused as previously described (Mackins et al., 2006). ALDH2*2 knock-in mice were donated by the Mochly-Rosen laboratory, Stanford University (Zambelli et al., 2014). Briefly, 20 min after a heparin i.p. injection (100 U) to avoid blood clotting, mice were anesthetized with CO_2 vapor and humanely killed by cervical dislocation while under anesthesia. Hearts were quickly excised and cooled in ice-cold Krebs-Henseleit (KH) solution containing pyruvic acid (2 mM) and equilibrated with 95% O_2 + 5% CO_2. Hearts were then perfused in a Langendorff apparatus (Radnoti, Monrovia, CA) at constant pressure (100 cm H_2O) at 37°C with KH buffer. After stabilization, hearts were subjected to 40-min global ischemia followed by 30-min reperfusion with KH buffer (I/R), reperfusion time was 120 min when I/R-induced infarct areas were analyzed. For IPC, hearts were subjected to 4 × 5-min cycles of ischemia each followed by 5-min perfusion. For pharmacologic prevention of IPC, hearts were pretreated with the selective $S1P_1R$ antagonist W146 (3 μM, 20 min) and then subjected to IPC (i.e., 4 × 5-min cycles of ischemia each followed by 5-min perfusion with W146). For pharmacologic preconditioning, hearts were perfused with the selective $S1P_1R$ agonist SEW2871 (0.1 μM)(Jo et al., 2005) for 4 × 5-min cycles, each followed by a 5-min washout before I/R. For prevention of pharmacologic precondition, $S1P_1R$ antagonist W146 (3 μM), PKCε inhibitor εV1-2 (1 μM) and ALDH2 desensitizer GTN (2 μM) were perfused for 20 min, before and during pharmacologic preconditioning and then washed out before I/R. ECG was recorded online (sample frequency of 1 kHz) and analyzed using Powerlab/8SP. Onset and duration of reperfusion arrhythmias were recorded and quantified according to the Lambeth

JPET Fast Forward. Published on May 12, 2017 as DOI: 10.1124/jpet.117.241976
This article has not been copyedited and formatted. The final version may differ from this version.

Conventions (Walker et al., 1988; Curtis et al., 2013).Coronary flow was measured by timed collections of the effluent every 2 min, samples were assayed for renin and NE.

Infarct size in WT and ALDH2*2 mouse hearts

WT and ALDH2*2 hearts were removed from the Langendorff apparatus after 120-min reperfusion. Hearts were cut in 2 mm-thick slices and immersed in an aqueous solution (1% w/v) of 2,3,5-Triphenyltetrazolium chloride (TTC, Sigma-Aldrich, St. Louis, MO, USA) for 20 min at 37°C and then in an aqueous solution of formaldehyde (10% v/v). After overnight incubation, heart slices were photographed with a X16 magnification and analyzed to measure infarct size (expressed as percentage of infarcted vs. total left ventricular area).

Cell lines

HMC-1 culture. The human mastocytoma cell line, HMC-1, was kindly provided by Dr. J. H. Butterfield (Mayo Clinic, Rochester, MN). Cells were maintained in suspension culture at high density in IMDM supplemented with 10% heat-inactivated FBS, 1% penicillin/streptomycin and kept at 37°C in a 5% CO_2 atmosphere (Aldi et al., 2015).

Bone marrow-derived MC (BMMC) culture. Bone marrow was collected from femurs and tibias of WT C57BL/6J mice (male, 10- to 12-week old, Jackson Laboratory, Bar Harbor, ME) and ALDH2*2 knock-in mice and euthanized by cervical dislocation under light CO_2 anesthesia, as approved by the Weill Cornell Medicine Institutional Animal Care and Use Committee. Bone marrow cells were cultured in RPMI 1640 medium (Invitrogen Life Technologies, Carlsbad, CA) containing 1% penicillin/streptomycin, 10% heat-inactivated fetal calf serum, 55 μM 2-mercaptoethanol, and recombinant murine IL-3 and SCF (PeproTech, Rocky Hill, NJ),

both at 20 ng/ml. Bone marrow cells were counted and placed in culture at a cell density of 5 x 10^5 cells/ml. Cell medium was changed every 3 to 4 days, and non-adherent cells were transferred to a new flask. Mature BMMC were obtained after 4 weeks of culture, and stained positive for Toluidine Blue; moreover, >90% of cells expressed both c-Kit and FcεRI. All experiments were performed with BMMC cultured for 4-7 weeks (Aldi et al., 2014a).

Immunofluorescence in BMMCs

Mature WT and ALDH2*2 BMMCs obtained after 4 weeks of culture were placed on poly-D-lysine-coated coverslips for 2 hours at 37°C to adhere. Cells were then washed with PBS, fixed with 4% PFA for 15 min at room temperature, washed in PBS and blocked in 1% BSA and 0.1% Triton-X-100 in PBS for 30 min. Then, cells were incubated overnight with mouse anti-$S1P_1R$ (Abcam, Cat. N° ab11424) and rat anti-c-Kit (Abcam, Cat N° ab65525). The following day, coverslips were washed with PBS and incubated with secondary Ab Alexa Fluor 488 donkey anti-rabbit IgG (green) and Alexa Fluor 594 rabbit anti-rabbit IgG (red). Nuclei were counterstained with DAPI 300 nM and coverslips were mounted on glass slides using VectaMount medium (Vector Laboratories, Burlingame, CA). Immunofluorescence images of cells were captured in a Z-stack with 1-µm steps using a Zeiss Axio Observer.Z1 microscope followed by deconvolution using the ZEN pro 2012 software (Carl Zeiss). To analyze the image we used ImagePro analyzer 7.0 software (Media Cybernetics).

Western blotting

To ascertain $S1P_1R$ expression in HMC-1, WT-BMMC and ALDH2*2-BMMC cells, we used an anti-$S1P_1R$ antibody purchased from Abcam (Cambridge, MA; rabbit monoclonal anti-EDG1, Cat. N° ab125074). Cells were lysed in ice-cold Lysis buffer

1X (Cell Signaling Technology, Danvers, MA). Proteins were equalized to the same concentration with the Bradford protein assay kit (Bio-Rad Laboratories, Hercules, CA), separated by SDS–PAGE and transferred to PVDF membranes. Membranes were blocked with 5% BSA dissolved in Tris-buffered saline containing 1% Tween 20 (TBST) for 1 h at room temperature. After washing with TBST, the membrane was incubated with a 1:10,000 dilution of specific antibody against $S1P_1R$ in 5% milk-TBST at 4°C overnight (antibody final concentration was 3.2 ng/ml). Blots were washed in TBST and the membranes were incubated in a 1:5,000 dilution of horseradish peroxidase-conjugated IgG secondary antibody (Cell Signaling Technology, Cat. N° 7074, final concentration 13 ng/ml) in 5% BSA-TBST at room temperature for 1 h. Total proteins were evaluated by incubating the PVDF membranes with a 1:50,000 dilution of β-actin HRP conjugated (Alpha Diagnostic International, San Antonio, TX, concentration 1 µg/ml) in milk 5% at room temperature. Proteins were detected using the ECL chemiluminescence system.

PKCε translocation

Following incubation of HMC-1, WT-BMMC and ALDH2*2-BMMC with PMA or SEW2871 for 10 min at 37°C, cytosolic and membrane fractions were prepared as previously described (Koda et al., 2010). When necessary, the $S1P_1R$ antagonist W146 was preincubated for 20 min at 37° C. Na^+/K^+ATPase antibody (Abcam, Cat. N° ab185065) was used for immunoblotting to verify the purity of the cell membrane fraction. Translocation of PKCε was determined by Western blot analysis using a PKCε antibody (Santa Cruz Biotechnology Inc., Santa Cruz, CA; Cat. N° sc-214) at a 1:1,000 dilution in 5% milk-TBST. Blots were washed in TBST and the membranes were incubated in a 1:5,000 dilution of goat anti-rabbit-IgG HRP secondary antibody (Cell Signaling Technology, Cat. N° 7074) in 5% milk-TBST at room temperature for 1

JPET Fast Forward. Published on May 12, 2017 as DOI: 10.1124/jpet.117.241976
This article has not been copyedited and formatted. The final version may differ from this version.

h. After washing with TBST, blots were developed by an ECL Western Blotting Detection Reagent and the membranes were exposed to Hyperfilm ECL. Total proteins were evaluated by incubating the PVDF membranes with a 1:50,000 dilution of β-actin HRP conjugated (Alpha Diagnostic International, San Antonio, TX, concentration 1 μg/ml) in milk 5% at room temperature. PKCε translocation was expressed as the ratio between PKCε in the membrane and PKCε in the cytosol. The density of each band was determined with GeneTool software.

ALDH2 Enzymatic Activity Assay.

Enzymatic activity of ALDH2 in HMC-1, WT-BMMC and ALDH2*2-BMMC cells was determined spectrophotometrically by monitoring the reductive reaction of NAD^+ to NADH at 340 nm as described previously (Koda et al., 2010). Briefly, cells were treated with SEW2871, Alda-1 or PMA for 10 min at 37° C. When indicated, $S1P_1R$ antagonist, PKCε and ALDH2 inhibitors were preincubated in the presence of SEW2871, for 20 min at 37° C. Cells were centrifuged at 2,500 rpm for 5 min at 4° C and pellets resuspended in homogenization buffer (composition: Tris-HCl pH=8 100 mM, DTT 10 mM, Glycerol 20%, Triton-X-100 1%). Assays were carried out in 50 mM sodium pyrophosphate buffer, pH 9.0, at 25°C, and 500 μg of cell lysates and 2.5 mM NAD were added to the buffer. To start the reaction, 10 mM acetaldehyde was added, and the accumulation of NADH was recorded for 15 min with measurements taken every 20 seconds. ALDH2 reaction rates were calculated as μmoles of NADH per min per mg of protein and compared with control cells [i.e., treated with Na Ringer (composition, mM: NaCl 154, KCl 5.61, $CaCl_2$ 2.16, $NaHCO_3$ 5.95 and dextrose 5.55)] and expressed as percent increase from control.

β-Hexosaminidase assay

β-Hexosaminidase (β-HEX) release was measured in HMC-1, WT-BMMC and ALDH2*2-BMMC. Briefly, cells were washed and resuspended in Ringer buffer. Identical volumes of cells were aliquoted in Eppendorf tubes (HMC-1) or in 96-well plates (BMMCs) and incubated with gentle oscillation at 37°C with acetaldehyde (300 and 100 μM for HMC-1 and BMMCs, respectively) or 4-HNE (30 and 10 μM, respectively) for 20 min (Sigma-Aldrich). When reported, HMC-1 and BMMC cells were treated with the $S1P_1R$ agonist SEW2871 at concentrations of 0.1 and 1 μM, respectively, for 10 min at 37°C. When required, HMC-1 and BMMCs were preincubated with the $S1P_1R$ antagonist (1 and 0.1 μM, respectively), PKCε (1 μM) and ALDH2 (2 μM) inhibitors for 20 min at 37° C. At the end of the incubation, samples were placed in ice and centrifuged at 500 x g for 5 min. Twenty μl of BMMC or HMC-1 supernatants were placed in 96-well plates, to which 50 μl of p-nitrophenyl-N-acetyl-β-D-glucosaminide (1.3 mg/ml dissolved in 0.1 M citrate buffer at pH 4.5) was added and incubated for 90 min at 37°C. Cell pellets were lysed with 0.5% Triton X-100, and total lysates were used to determine total β-HEX content. The reaction was stopped by adding 150 μl of 0.2 M glycine (pH 10.7). Optical density was read at 405 nm on a spectrophotometric plate reader using SoftMax Pro version 4.8 (Molecular Devices, Sunnyvale, CA). β-HEX release was expressed as percent of total β-HEX (where total β-HEX denotes the sum of β-HEX in supernatant and total cell lysate)(Aldi et al., 2014a).

Renin assay

For the renin assay, human and porcine angiotensinogen was used for HMC-1 and BMMC samples, respectively. Renin activity, in terms of angiotensin I (Ang I)

formed, was determined by GammaCoat Plasma Renin Activity [^{125}I] Radioimmunoassay (DiaSorin, Stillwater, MN). Cell pellets were lysed with cell lysis buffer 1X (Cell Signaling Technology), and total lysates were used to determine total protein concentration by the Bradford Protein Assay kit (Bio-Rad Laboratories). Total protein concentration was used to normalize renin release. Results were expressed as percent increase above basal level.

Statistics

Statistical analysis was performed with GraphPad Prism 6.0 software (San Diego, CA, USA). All data are reported as means ± SEM. Statistical analysis was performed only when a minimum of n = 5 independent samples was acquired, and was performed with unpaired *t*-test when comparing two different groups and with one-way ANOVA followed by Dunnett's post-hoc test when comparing more than two groups of data (Figure 5). Data and statistical analysis comply with the recommendations on experimental design and analysis in pharmacology (Curtis et al., 2015). Data were considered statistically significant when a value of at least $p<0.05$ was achieved.

Study approval

All animals were kept in the animal care facility under controlled temperature, humidity and light/dark cycle, with food and water *ad libitum*. All animal procedures were carried out in accordance with the Guide for the Care and Use of Laboratory Animals as adopted and promulgated by the U.S. National Institutes of Health, and were approved by the Weill Cornell Medicine Institutional Animal Care and Use Committee.

Results

$S1P_1R$ activation mimics IPC and affords anti-RAS cardioprotection in isolated guinea-pig hearts

Since guinea pig hearts share more similarity with human hearts and represent a better and a more relevant clinical model (Choy et al., 2016), and also given our previous experience with other G_i-coupled receptors in this animal model (Koda et al., 2010; Aldi et al., 2014b), initial experiments were performed in isolated guinea-pig hearts. Spontaneously beating Langendorff-perfused guinea pig hearts were subjected to 20-min global ischemia followed by 30-min reperfusion (I/R). We had previously shown that I/R results in MC degranulation, demonstrated by a 2-fold increase in β-hexosaminidase (β-HEX) overflow into the coronary effluent (Koda et al., 2010). I/R also caused large increases in renin and NE overflow (i.e., ~4- and ~200-fold, respectively), and severe ventricular arrhythmias (tachycardia and fibrillation, VT/VF) that lasted ~7 min (Figure 1). We had previously shown that the enhanced NE overflow and arrhythmias caused by I/R result from the activation of a local RAS by renin released from cardiac MCs (Mackins et al., 2006).

When I/R was preceded by a 20-min perfusion with the selective $S1P_1R$ antagonist W146 (1 μM)(Gonzalez-Cabrera et al., 2008) followed by a 10-min washout, the overflows of renin and NE were each enhanced ~1.8-fold and the duration of VT/VF was extended ~1.4 fold (Figure 1), clearly indicating that $S1P_1R$ blockade exacerbates the effects of I/R-induced activation of a local cardiac RAS, and suggesting that $S1P_1R$ may play a cardioprotective anti-RAS role.

We had previously shown that IPC affords anti-RAS cardioprotection by stabilizing MCs in the heart prior to I/R (Koda et al., 2010). Since endogenously produced S1P is a mediator of IPC (Vessey et al., 2009), and MCs express $S1P_1R$

JPET Fast Forward. Published on May 12, 2017 as DOI: 10.1124/jpet.117.241976
This article has not been copyedited and formatted. The final version may differ from this version.

(Jolly et al., 2004), we next assessed whether selective pharmacologic blockade of $S1P_1R$ in the heart counteracts the IPC-mediated attenuation of renin release in hearts subjected to I/R. We found that two 5-min cycles of ischemia, each followed by 5-min reperfusion (IPC)(Koda et al., 2010), decreased the I/R-induced renin and NE overflow by ~2.8- and ~1.6-fold, respectively, and also reduced by one half the duration of VT/VF (Figure 1). Notably, selective blockade of $S1P_1R$ with W146 (1 μM), prevented these anti-RAS effects of IPC, in that renin and NE overflow, and VT/VF duration in IPC hearts with $S1P_1R$ blockade did not differ from those in hearts subjected to I/R alone (Figure 1). Similarly, with $S1P_1R$ blockade these parameters did not differ from those in hearts subjected to I/R alone (Figure 1).

We next perfused hearts with the selective $S1P_1R$ agonist SEW2871 (Jo et al., 2005) (1 μM, for two 5-min cycles each followed by 5-min washout) prior to I/R. Pre-perfusion with SEW2871 mimicked the protective effects of IPC, in terms of renin and NE overflow and VT/VF duration, which were reduced as much as by IPC (Figure 1). Notably, this protective effect of SEW2871 was prevented by selective blockade of $S1P_1R$ with compound W146 (1 μM) (Figure 1). These results indicated that $S1P_1R$ activation likely plays a role in the cardioprotective anti-RAS effects of IPC.

PKCε and ALDH2 mediate the protective IPC-like anti-RAS effects of $S1P_1R$ activation in isolated guinea-pig hearts

We had previously shown that PKCε activation/translocation is involved in the cardioprotective anti-RAS effects of IPC (Koda et al., 2010). Accordingly, we next investigated the role of PKCε in the cardioprotective anti-RAS effects of $S1P_1R$ activation. We found that selective inhibition of PKCε with compound εV_{1-2} (Johnson et al., 1996) (1 μM) prevented the IPC-like cardioprotective anti-RAS effects of $S1P_1R$

JPET Fast Forward. Published on May 12, 2017 as DOI: 10.1124/jpet.117.241976
This article has not been copyedited and formatted. The final version may differ from this version.

activation (i.e., compound $\varepsilon V_{1\text{-}2}$ abolished the SEW2871-induced inhibition of renin and NE release as well as the alleviation of VT/VF; Figure 1).

We next assessed whether the anti-RAS effect of $S1P_1R$ activation also involve ALDH2 activation. For this, we investigated whether inhibition/inactivation of ALDH2 would abolish the anti-RAS effects of $S1P_1R$ activation. We found that nitroglycerine (GTN), perfused for 30 min before I/R at a concentration (2 μM) which is known to inactivate ALDH2 (Chen et al., 2008), prevented the IPC-like cardioprotective anti-RAS effects of $S1P_1R$ activation (i.e., GTN abolished the SEW2871-induced inhibition of renin and NE release as well as the alleviation of VT/VF; Figure 1). Thus, activation of both ALDH2 and PKCε appears to be required for the genesis of the IPC-like cardioprotective anti-RAS effects of $S1P_1R$ activation.

Lack of IPC- and $S1P_1R$-mediated anti-RAS protection in ALDH2*2 knock-in mouse hearts

As a negative control, we used a heart model of I/R and I/R preceded by IPC from knock-in mice, in which ALDH2 activity is dramatically reduced (Zambelli et al., 2014). Spontaneously beating Langendorff-perfused wild-type (WT) mouse hearts were subjected to 30-min normothermic global ischemia followed by 40-min reperfusion. I/R in the WT *ex-vivo* mouse heart resulted in large increases in renin and NE overflow (i.e., ~60- and ~100-fold compared to basal control, respectively), and severe ventricular arrhythmias (VT/VF) that lasted ~2 min (Figure 2). We had previously shown that the enhanced NE overflow and arrhythmias in the mouse heart exposed to I/R result from the activation of a local RAS initiated by renin released from cardiac MC (Mackins et al., 2006; Aldi et al., 2014b). When mouse hearts were subjected to IPC (i.e., 4 x 5-min cycles of ischemia each followed by 5-min reperfusion)

prior to I/R, renin and NE overflow were reduced ~3.5- and ~3-fold, respectively, and VT/VF duration was reduced ~2.5 fold (Figure 2). Notably, when WT mouse hearts were pretreated with the selective $S1P_1R$ antagonist W146 (3 μM, 20 min) and then subjected to IPC, the cardioprotective anti-RAS effects of IPC were abolished (Figure 2).

Another group of WT mouse hearts were perfused with the $S1P_1R$ agonist SEW2871 (0.1 μM) for 4 x 5-min cycles, each followed by a 5-min washout before I/R. Similar to what observed in guinea pig hearts (see Figure 1), we found that activation of $S1P_1R$ with SEW2871 mimicked the cardioprotective anti-RAS effects of IPC (Figure 2). Notably, this IPC-like anti-RAS effect was prevented in WT mouse hearts pretreated with the selective $S1P_1R$ antagonist W146 (3 μM, 20 min) (Figure 2). Moreover, the IPC-like anti-RAS effect was prevented in WT mouse hearts pretreated with the selective PKCε inhibitor compound εV_{1-2} (1 μM; 20 min) or the ALDH2 inactivator GTN (2 μM; 30 min) (Figure 2).

Thus, the anti-RAS cardioprotective effects of IPC and $S1P_1R$ activation observed in mouse hearts were similar to those observed in guinea-pig hearts, in which ALDH2 activation appeared to play a pivotal role. Hence, to solidify the notion that ALDH2 activation plays a major role in the anti-RAS cardioprotection afforded by IPC and $S1P_1R$, we used the recently developed ALDH2*2 knock-in mouse model, in which ALDH2 enzymatic activity is radically reduced (Zambelli et al., 2014). We found that either IPC or SEW2871 pretreatment (0.1 μM; 4 x 5-min cycles) failed to protect ALDH2*2 hearts, in terms of renin and NE overflow, and duration of arrhythmias. In fact, preconditioned and SEW2871-pretreated ALDH2*2 hearts did not differ from ALDH2*2 hearts subjected to I/R alone (Figure 2). Nor any difference was found when ALDH2*2 hearts were pretreated with the selective $S1P_1R$ antagonist, the selective

JPET Fast Forward. Published on May 12, 2017 as DOI: 10.1124/jpet.117.241976
This article has not been copyedited and formatted. The final version may differ from this version.

PKCε inhibitor compound εV_{1-2} or the ALDH2 inactivator GTN (Figure 2). These findings corroborated the notion that full ALDH2 enzymatic activity is needed to elicit the anti-RAS cardioprotection afforded by either IPC or $S1P_1R$ activation.

IPC- and $S1P_1R$ activation fail to reduce infarct size in ALDH2*2 knock-in mouse hearts

The size of ventricular tissue exhibiting evidence of I/R-induced cell death is widely used as a suitable indicator of I/R-induced injury (Fishbein et al., 1981; Chen et al., 2008; Redfors et al., 2012). Further, angiotensin II (Ang II) formed upon RAS activation is known to generate oxygen radicals, which contribute to ischemic heart damage (Mehta and Griendling, 2007; Wen et al., 2012; Balakumar and Jagadeesh, 2014). Therefore, to test further potential cardioprotective effects of $S1P_1R$ activation and their possible dependence on ALDH2 activity, we measured infarct size in Langendorff-perfused mouse hearts preconditioned with IPC or treated with the selective $S1P_1R$ agonist (SEW2871, 0.1 μM), in the presence or absence of the $S1P_1R$ antagonist (W146, 3 μM). We found that following 40-min ischemia/2-h reperfusion, ventricular infarcted area amounted to ~40% of the entire area in hearts from both WT and ALDH2*2 mice (Figure 3A and B). Notably, either IPC (4 x 5-min cycles) or $S1P_1R$ activation (4 x 5-min cycles of SEW2871, 0.1 μM) reduced infarct size in WT hearts by ~75 and ~60 %, respectively. In contrast, no reduction in infarct size was observed when ALDH2*2 hearts were ischemically preconditioned or perfused with the $S1P_1R$ agonist, either alone or in the presence of the $S1P_1R$ antagonist (Figure 3A and B). These findings suggested that ALDH2 plays a role not only in the anti-RAS cardioprotection afforded by either IPC or $S1P_1R$ activation, but also in the IPC- or $S1P_1R$-induced reduction of infarct size.

JPET Fast Forward. Published on May 12, 2017 as DOI: 10.1124/jpet.117.241976
This article has not been copyedited and formatted. The final version may differ from this version.

MCs express $S1P_1R$

Given the pivotal role that local MCs play in the activation of RAS in the heart (Mackins et al., 2006), MCs are the probable site at which the IPC-like anti-RAS effects of $S1P_1R$ activation develop. Thus, we first ascertained by Western immunoblot analysis that HMC-1, WT-BMMC and ALDH2*2-BMMC all express $S1P_1R$ (Figure 4A). Even though it had already been demonstrated that human LAD2 MC, cord blood–derived human MC (Oskeritzian et al., 2008), WT-BMMC and RBL-2H3 all express $S1P_1R$ (Jolly et al., 2004), here we show for the first time that the $S1P_1R$ is expressed in ALDH2*2-BMMC. To corroborate the presence of $S1P_1R$ in MCs we used a triple staining technique for mature MCs (red), $S1P_1R$ (green) and nuclei (blue) (Figure 4B). Clearly, when compared with WT-BMMC, ALDH2*2-BMMC showed neither a lack nor a diminished expression of the receptor, both with immunoblot and immunocytochemistry analysis. This indicates that the lack of $S1P_1R$-induced anti-RAS cardioprotection in ALDH2*2 hearts (see Figure 2 and 3), as well as the failure of the $S1P_1R$ agonist to activate ALDH2 in ALDH2*2 BMMC (see Figure 5), is not due to a diminished expression of $S1P_1R$ in MCs.

$S1P_1R$ activation translocates/activates PKCε in MCs

Having found that the cardioprotective anti-RAS effects of $S1P_1R$ activation are ALDH2-dependent and prevented by PKCε inhibition, and that $S1P_1R$ are expressed in MCs, we hypothesized that MCs are the site at which the IPC-like effects of $S1P_1R$ activation are initiated and mediated by PKCε and ALDH2 activation. Thus, we next ascertained that MC PKCε is translocated/activated upon $S1P_1R$ activation. Utilizing Western analysis in cytosolic and membrane fractions of HMC-1 and BMMC cells, we found that the phorbol ester PMA (10 nM; positive control) markedly increased the

JPET Fast Forward. Published on May 12, 2017 as DOI: 10.1124/jpet.117.241976
This article has not been copyedited and formatted. The final version may differ from this version.

translocation of PKCε from cytosol to membrane (i.e., a hallmark of PKCε activation) (Figure 4C and D). Incubation of HMC-1 and BMMC cells with the $S1P_1R$ agonist (SEW2871, 1 and 0.1 μM, respectively, for 10 min) also enhanced PKCε translocation from cytosol to membrane, an effect which was blocked by preincubation with the $S1P_1R$ antagonist W146 (1 and 0.1 μM, respectively, for 20 min) (Figure 4C and D). Similarly, PKC and $S1P_1R$ activation each enhanced PKCε translocation in BMMC from ALDH2*2 mice (Figure 4E), a process that was prevented by $S1P_1R$ blockade. This indicates that $S1P_1R$-induced PKCε translocation/activation in MCs is independent of ALDH2.

$S1P_1R$ activation enhances ALDH2 activity in MCs

Our findings in guinea-pig and mouse hearts *ex vivo* suggested that ALDH2 mediates the anti-RAS, IPC-like effects of $S1P_1R$ activation (see Figures 1 and 2); thus, we next assessed whether $S1P_1R$ activation in MC elicits an increase in ALDH2 activity. For this, we measured ALDH2 activity in HMC-1 and BMMC cells in response to the $S1P_1R$ agonist SEW2871. We found that in both HMC-1 and WT-BMMC, SEW2871 (1 and 0.1 μM, respectively, 10 min) elicited a ~30% increase in ALDH2 enzymatic activity (i.e., NADH production), comparable to that induced by the specific ALDH2 activator Alda-1 (300 μM, 10 min)(Budas et al., 2009) used as positive control (Figure 5A and B). Notably, the $S1P_1R$-induced increase in ALDH2 activity was prevented by the $S1P_1R$ antagonist W146 (1 and 0.1 μM, respectively, 20 min), by the selective ALDH2 inactivator GTN (2 μM, 25 min) (Koda et al., 2010) and by the PKCε inhibitor compound $\varepsilon V_{1\text{-}2}$ (1 μM, 20 min) (Figure 5A and B). This suggested that activation of PKCε is necessary for the $S1P_1R$-induced increase in ALDH2 activity. In

JPET Fast Forward. Published on May 12, 2017 as DOI: 10.1124/jpet.117.241976
This article has not been copyedited and formatted. The final version may differ from this version.

fact, the general PKC activator PMA (300 and 10 nM, 10 min) also significantly increased NADH production in HMC-1 and WT-BMMC (Figure 5A and B).

As a negative control, we investigated the effects of Alda-1, PMA and SEW2871 in BMMC obtained from ALDH2*2 mice: we found that none of these compounds elicited a significant change in ALDH2 activity; nor was ALDH2 activity changed when the $S1P_1R$ agonist was used in the presence of its antagonist, of the PKCε inhibitor or the ALDH2 inactivator (Figure 4C).

$S1P_1R$ activation inhibits MC degranulation and renin release elicited by acetaldehyde: dependence on ALDH2.

We next investigated the role of ALDH2 in MC degranulation and renin release elicited by acetaldehyde, a prototypic toxic compound that accumulates during I/R (Chen et al., 2008; Koda et al., 2010). First, by comparing WT-BMMC with ALDH2*2-BMMC, we correlated the level of ALDH2 activity with the extent of inhibition of acetaldehyde-induced MC degranulation and renin release. We found that the selective ALDH2 activator Alda-1 (300 μM) enhanced ALDH2 activity by 60% in WT-BMMC, while it failed to affect it in ALDH2*2-BMMC (Figure 6A and B). At the same time, Alda-1 (20 μM) markedly inhibited acetaldehyde-induced degranulation and renin release in WT-BMMC, while it failed to affect it in ALDH2*2-BMMC (Figure 6C and D). This indicates that a fully functioning ALDH2 is a prerequisite for the inhibition of acetaldehyde-induced MC degranulation and associated renin release.

We next assessed whether $S1P_1R$ activation inhibits acetaldehyde-induced MC degranulation and renin release, and we also investigated the role played by PKC_ε and ALDH2 in this action. We found that $S1P_1R$ activation with SEW2871 (1 and 0.1 μM, respectively) inhibited acetaldehyde-induced degranulation and renin release in

JPET Fast Forward. Published on May 12, 2017 as DOI: 10.1124/jpet.117.241976
This article has not been copyedited and formatted. The final version may differ from this version.

HMC-1 and WT-BMMC; this effect was prevented by the $S1P_1R$ antagonist W146 (1 and 0.1 μM, respectively)(Figure 7A and B). In contrast, $S1P_1R$ activation did not affect acetaldehyde-induced degranulation and renin release in ALDH2*2-BMMC (Figure 7C), indicating the indispensable role of ALDH2 in the $S1P_1R$-induced prevention of degranulation and renin release elicited by acetaldehyde. Notably, the selective PKC_ε inhibitor, εV1-2, and the ALDH2 inactivator, GTN, each prevented the SEW2871-induced abolition of acetaldehyde-induced MC degranulation and renin release in HMC-1, WT-BMMC and ALDH2*2-BMMC cells (Figure 7). Collectively, these findings indicate that activation of $S1P_1R$ on the MC membrane leads sequentially to $PKC\varepsilon$ translocation and ALDH2 activation, which prevents the degranulating effects of acetaldehyde, known to be produced in I/R.

Similar to acetaldehyde, 4-hydroxynonenal (4-HNE) is another toxic compound produced in large quantities during oxidative stress (Esterbauer et al., 1991; Eaton et al., 1999; Kaludercic et al., 2014). 4-HNE also elicited BMMC degranulation and renin release that were markedly reduced by the $S1P_1R$ agonist SEW2871; this effect was abolished by the $S1P_1R$ antagonist W146 (Figure 8). Notably, SEW2871 failed to inhibit BMMC degranulation and renin release in BMMC from ALDH2*2 animals (Figure 8).

JPET Fast Forward. Published on May 12, 2017 as DOI: 10.1124/jpet.117.241976
This article has not been copyedited and formatted. The final version may differ from this version.

Discussion

Our results clearly show that activation of $S1P_1R$ on the MC membrane during I/R affords cardioprotective anti-RAS effects, which -similar to IPC- include a reduction of renin and NE release, and alleviation of reperfusion arrhythmias. Activation of ALDH2 in MC plays a pivotal role in this cardioprotection.

MC number increases in ischemic canine and human hearts (Frangogiannis et al., 1998; Patella et al., 1998). Cardiac MC synthesize renin, which is released in enzymatically active form in I/R and promotes the activation of a local RAS, culminating in enhanced NE release and VT/VF (Silver et al., 2004; Mackins et al., 2006). Notably, in the absence of cardiac MC (i.e., c-Kit knockout mice), renin immunoreactivity disappears, and I/R fails to activate a local RAS and to elicit VT/VF (Mackins et al., 2006). In previous studies we reported that cardiac MC degranulation by toxic aldehydes produced during I/R was inhibited by ALDH2 activation, either directly, via selective ALDH2 activators (i.e., Alda-1), or via stimulation of G_i-coupled A_3 and H_4-receptors with adenosine and histamine, respectively. This process afforded a MC-mediated anti-RAS cardioprotection (Koda et al., 2010; Aldi et al., 2014b). Accordingly, we questioned whether the stimulation of other G_i-coupled receptors expressed on MC, and the consequent activation of mitochondrial ALDH2, might provide similar protective IPC-like effects in I/R.

We focused on $S1P_1R$ because these receptors are G_i-coupled (Means and Brown, 2009), are found to be present in the rat and mouse hearts (Egom et al., 2010; Keul et al., 2016), and in RBL-2H3 MC lines (Jolly et al., 2004). MC $S1P_1R$ are plausibly activatable by their natural endogenous ligand (i.e., S1P), known to be made in the I/R heart (Means and Brown, 2009) and in MC themselves (Obinata and Hla, 2012). In fact, MC-derived S1P might well elicit “inside-out” effects (Takabe et al.,

2008). In support of the hypothesis that $S1P_1R$ might provide protective IPC-like anti-RAS effects in I/R, we found that pharmacologic blockade of $S1P_1R$ with the selective antagonist W146 (Gonzalez-Cabrera et al., 2008) prevents the protective effects of IPC in cavian and murine hearts, indicating that functional $S1P_1R$ are indispensable for the development of the anti-RAS effects of IPC. This notion is corroborated by the discovery that pharmacologic activation of $S1P_1R$ with the selective agonist SEW2871 (Jo et al., 2005) mimics the anti-RAS effects of IPC in both cavian and murine hearts, as shown by a marked reduction of renin and NE release and alleviation of arrhythmias. A definitive MC involvement was proven by the finding that pharmacologic activation of $S1P_1R$ in cultured human and murine MC prevented degranulation and renin release elicited by acetaldehyde and 4-HNE, two characteristic endogenous products of I/R (Chen et al., 2008). It is noteworthy that this protective effect was prevented by pharmacologic $S1P_1R$ blockade.

Moreover, we found that, not only IPC, but also the administration of the $S1P_1R$ agonist SEW2871, markedly reduced the I/R-induced left ventricular infarct size in a murine *ex vivo* model. In contrast, infarct size increased when treatment with SEW2871 was preceded by the administration of the selective $S1P_1R$ antagonist W146. Blockade of IPC-induced protection against ischemic injury had been previously observed with a $S1P_1R$ antagonist in the I/R rat heart (Vessey et al., 2009), while deletion of $S1P_1R$ in mouse myocytes was found to be associated with ischemic injury due to an impaired phosphorylation of the Akt survival kinase pathway, disruption of intracellular Ca^{2+} homeostasis and NHE activity (Keul et al., 2016). In addition, Akt phosphorylation, as a mechanism of preconditioning, did not occur in a sphingosine kinase 1–deficient mice ($Sphk1^{-/-}$) (Jin et al., 2004), suggesting that $S1P_1R$ activation exerts cardioprotective effects through Akt. Thus, $S1P_1R$ stimulation

appears to protect the heart not only from the severe arrhythmias due to RAS activation, but also from ischemic injury, probably due to different mechanisms possibly initiated by the activation of $S1P_1R$ on cardiomyocytes.

Yet, Ang II generated upon RAS activation can lead to the formation of reactive oxygen species, which are likely contributors to ischemic heart damage (Mehta and Griendling, 2007; Wen et al., 2012; Balakumar and Jagadeesh, 2014). Hence the $S1P_1R$-induced reduction of infarct size can still be part of the overall anti-RAS cardioprotection. Recently, activation of S1P receptor subtype 3 ($S1P_3R$) was found to protect against ischemia/reperfusion (Yung et al., 2017), suggesting that therapeutic benefits in ischemic heart disease could be provided by activating both $S1P_1R$ and $S1P_3R$.

Intrigued by these $S1P_1R$-mediated anti-RAS protective effects, we next investigated their signaling mechanisms. Given that G_i-coupled receptors are known to translocate/activate PKCε (Inagaki et al., 2006), probably via phospholipase C-diacylglycerol activation (Takai et al., 1979), we asked whether PKCε inhibition would preclude the effects of $S1P_1R$ activation. We found that PKCε inhibition with compound εV_{1-2} (Johnson et al., 1996) not only abolished the IPC-like anti-RAS effects of $S1P_1R$ activation with SEW2871 (Jo et al., 2005) in cavian and murine hearts, but also prevented SEW2871 from attenuating the degranulating and renin-releasing effects of acetaldehyde and 4-HNE in cultured human and murine MC, clearly indicating an involvement of PKCε in the anti-RAS effects of SEW2871.

Indeed, SEW2871 translocated/activated PKCε from cytosol to membrane in HMC-1 and BMMC, confirming that the cardioprotective effects of $S1P_1R$ activation depend on the translocation/activation of PKCε. PKCε is known to phosphorylate mitochondrial ALDH2 in cardiac myocytes (Chen et al., 2008), while in MC ALDH2

phosphorylation has been shown to prevent the MC-degranulating and renin-releasing effects of reactive oxygen species and toxic aldehydes (Koda et al., 2010; Aldi et al., 2014b). Hence, to uncover the relevance of ALDH2, we pre-empted its action with an excess of GTN (Koda et al., 2010). Similar to PKCε blockade, ALDH2 inhibition abolished the protective anti-RAS effects of IPC in *ex-vivo* hearts and prevented SEW2871 from attenuating the degranulating and renin-releasing effects of acetaldehyde in both HMC-1 and BMMC. It is noteworthy that PKCε blockade prevented ALDH2 activation by SEW2871.

Most importantly, either IPC or $S1P_1R$ activation failed to elicit anti-RAS cardioprotection in *ex-vivo* hearts excised from ALDH2*2 mice, engineered to practically lack ALDH2 activity (Zambelli et al., 2014). In *in-vitro* experiments on BMMC cultured from ALDH2*2 mice, we found that $S1P_1R$ is equally expressed on MC membranes from ALDH2*2 and WT mice. Moreover, we showed that the selective ALDH2 activator Alda-1 (Chen et al., 2008) did not activate ALDH2 in ALDH2*2 BMMC and that SEW2871 also failed to activate ALDH2 in the same cells. Nevertheless, SEW2871 was capable of translocating/activating PKCε in ALDH2*2 BMMC, indicating that this is a necessary step for ALDH2 activation, since it is preserved even when ALDH2 is non-functioning. Notably, in ALDH2*2 BMMC, as opposed to WT BMMC, ALDH2 activation with Alda-1 did not prevent acetaldehyde-induced degranulation and renin release. Similarly, $S1P_1R$ activation markedly reduced 4-HNE-induced degranulation and renin release in WT BMMC but not in ALDH2*2 BMMC; furthermore, infarct size in *ex-vivo* ALDH2*2 hearts was not reduced by S1P1R activation, demonstrating the pivotal role of MC ALDH2 in anti-RAS cardioprotection.

Collectively, these findings indicate that the IPC-like $S1P_1R$-mediated inhibition of I/R-induced cardiac MC degranulation and renin release results from an initial

translocation of PKCε and subsequent phosphorylation of ALDH2, culminating in the elimination of the MC degranulating effects of acetaldehyde and other toxic species produced during I/R (see Figure 9). Although we did not measure translocation of PKCε to cardiac mitochondria, work by the Mochly-Rosen laboratory has demonstrated that PKCε activates the intramitochondrial enzyme ALDH2 in an *ex-vivo* model of myocardial infarction. This protection coincides with the translocation of PKCε to cardiac mitochondria, where it associates with ALDH2 (Chen et al., 2008; Churchill et al., 2009). Importantly, as mentioned above, we found that in hearts and BMMCs from ALDH2*2 mice, no protective anti-RAS effects of IPC occurred, nor $S1P_1R$-mediated ALDH2 activation, even though PKCε was still activatable with PMA and/or with the $S1P_1R$ agonist.

Interestingly, I/R leads to monoamine oxidase (MAO) activation (Kaludercic et al., 2011). MAO is also expressed in MC (Vitalis et al., 2003) and contributes to the generation of H_2O_2 and toxic aldehydes (Bianchi et al., 2005). Moreover, it was recently demonstrated that inhibition of ALDH2 by small interfering RNA, in combination with MAO activation, leads to mitochondrial dysfunction and cell death in heart failure (Kaludercic et al., 2010; Kaludercic et al., 2014). Accordingly, $S1P_1R$-induced ALDH2 activation could play an additional cardioprotective role by decreasing MAO-produced toxic aldehydes and preventing myocardial damage.

Conclusions

Our collective evidence delineates a novel cardioprotective role for $S1P_1R$ on the MC membrane. Their direct pharmacological activation by selective agonists and/or in an autocrine mode by MC-derived S1P (i.e., by “inside-out” signaling) (Takabe et al., 2008) leads sequentially to PKC_ε and ALDH2 activation, reduction of

toxic aldehyde-induced MC degranulation, decreased renin release, prevention of RAS activation, reduction of NE release, and ultimately alleviation of reperfusion arrhythmias (see Figure 9). Moreover, $S1P_1R$ activation mimics IPC in reducing infarct size in hearts isolated from WT but not from ALDH2*2 mice.

Aside from the physiologic and pathophysiologic relevance of this newly discovered protective pathway, our findings suggest that MC $S1P_1R$ may represent a new pharmacologic and therapeutic target for the direct alleviation of RAS-induced cardiac dysfunctions, including ischemic heart disease and congestive heart failure. It is noteworthy that $S1P_1R$ could also grant cardioprotection by additional mechanisms initiated by the activation of $S1P_1R$ on cardiomyocytes (Jin et al., 2004; Keul et al., 2016) and sympathetic nerve endings. Indeed, PC12 cells, a known model of sympathetic nerve endings (Greene and Tischler, 1976), express $S1P_1R$ (Safarian et al., 2015). Being G_i-coupled (Means and Brown, 2009), $S1P_1R$ could likely inhibit NE release from cardiac sympathetic nerves, as other G_i-coupled receptors do (Levi et al., 2007). This effect could complement the reduction of NE release ultimately resulting from $S1P_1R$ -mediated actions at the MC level. Yet, we had found that when hearts of MC-deleted mice are exposed to I/R, renin release and VT/VF are abolished (Mackins et al., 2006). This supports the notion that MC, and MC-expressed $S1P_1R$, are essential for the anti-RAS cardioprotective effects of $S1P_1R$ activation.

Lastly, in addition to the heart, $S1P_1R$-mediated protective mechanisms may impact other organs (e.g., brain, liver, and kidney) that have renin-containing MC (Reid et al., 2007; Biran et al., 2008; Veerappan et al., 2008), can suffer ischemic episodes (Kaneko et al., 1998; Guo et al., 2004; Chen et al., 2009), and have been shown to be protected by IPC (Nandagopal et al., 2001; Adachi et al., 2006; Koda et al., 2010; Kukreja, 2012).

Acknowledgments.

We thank Dr. Annarita Di Lorenzo for her expert assistance and advice.

Authorship Contributions.

Partecipated in research design: Marino, Robador and Levi.

Conducted experiments and performed data analysis: Marino, Sakamoto, Robador, Tomita and Levi.

Wrote the manuscript: Levi and Marino

Contributed to edit the manuscript: Marino, Sakamoto, Robador, Tomita and Levi

References

Adachi N, Liu K, Motoki A, Nishibori M and Arai T (2006) Suppression of ischemia/reperfusion liver injury by histamine H4 receptor stimulation in rats. *Eur J Pharmacol* **544**:181-187.

Airaksinen KE (1999) Autonomic mechanisms and sudden death after abrupt coronary occlusion. *Ann Med* **31**:240-245.

Aldi S, Marino A, Tomita K, Corti F, Anand R, Olson KE, Marcus AJ and Levi R (2015) E-NTPDase1/CD39 modulates renin release from heart mast cells during ischemia/reperfusion: a novel cardioprotective role. *FASEB J* **29**:61-69.

Aldi S, Robador PA, Tomita K, Di Lorenzo A and Levi R (2014a) IgE receptor-mediated mast-cell renin release. *Am J Pathol* **184**:376-381.

Aldi S, Takano KI, Tomita K, Koda K, Chan NY, Marino A, Salazar-Rodriguez M, Thurmond RL and Levi R (2014b) Histamine H4-receptors inhibit mast cell renin release in ischemia/reperfusion via protein kinase Ce-dependent aldehyde dehydrogenase type-2 activation. *J Pharmacol Exp Ther* **349**:508-517.

Balakumar P and Jagadeesh G (2014) A century old renin-angiotensin system still grows with endless possibilities: AT receptor signaling cascades in cardiovascular physiopathology. *Cell Signal* **26**:2147-2160.

Bianchi P, Kunduzova O, Masini E, Cambon C, Bani D, Raimondi L, Seguelas MH, Nistri S, Colucci W, Leducq N and Parini A (2005) Oxidative stress by monoamine oxidase mediates receptor-independent cardiomyocyte apoptosis by serotonin and postischemic myocardial injury. *Circulation* **112**:3297-3305.

Biran V, Cochois V, Karroubi A, Arrang JM, Charriaut-Marlangue C and Heron A (2008) Stroke induces histamine accumulation and mast cell degranulation in the neonatal rat brain. *Brain Pathol* **18**:1-9.

Budas GR, Disatnik MH and Mochly-Rosen D (2009) Aldehyde dehydrogenase 2 in cardiac protection: a new therapeutic target? *Trends Cardiovasc Med* **19**:158-164.

Chen CH, Budas GR, Churchill EN, Disatnik MH, Hurley TD and Mochly-Rosen D (2008) Activation of aldehyde dehydrogenase-2 reduces ischemic damage to the heart. *Science* **321**:1493-1495.

Chen PS, Chen LS, Cao JM, Sharifi B, Karagueuzian HS and Fishbein MC (2001) Sympathetic nerve sprouting, electrical remodeling and the mechanisms of sudden cardiac death. *Cardiovasc Res* **50**:409-416.

Chen S, Li G, Zhang W, Wang J, Sigmund CD, Olson JE and Chen Y (2009) Ischemia induced brain damage is enhanced in human renin and angiotensinogen double transgenic mice. *Am J Physiol Regul Integr Comp Physiol* **297**:R1526-R1531.

Choy L, Yeo JM, Tse V, Chan SP and Tse G (2016) Cardiac disease and arrhythmogenesis: Mechanistic insights from mouse models. *Int J Cardiol Heart Vasc* **12**:1-10.

Churchill EN, Disatnik MH and Mochly-Rosen D (2009) Time-dependent and ethanol-induced cardiac protection from ischemia mediated by mitochondrial translocation of varepsilonPKC and activation of aldehyde dehydrogenase 2. *J Mol Cell Cardiol* **46**:278-284.

Curtis MJ, Bond RA, Spina D, Ahluwalia A, Alexander SP, Giembycz MA, Gilchrist A, Hoyer D, Insel PA, Izzo AA, Lawrence AJ, MacEwan DJ, Moon LD, Wonnacott S, Weston AH and McGrath JC (2015) Experimental design and analysis and their reporting: new guidance for publication in BJP. *Br J Pharmacol* **172**:3461-3471.

Curtis MJ, Hancox JC, Farkas A, Wainwright CL, Stables CL, Saint DA, Clements-Jewery H, Lambiase PD, Billman GE, Janse MJ, Pugsley MK, Ng GA, Roden DM, Camm AJ and Walker MJ (2013) The Lambeth Conventions (II): Guidelines for the study of animal and human ventricular and supraventricular arrhythmias. *Pharmacol Ther* **139**:213-248.

Eaton P, Li JM, Hearse DJ and Shattock MJ (1999) Formation of 4-hydroxy-2-nonenal-modified proteins in ischemic rat heart. *Am J Physiol* **276**:H935-H943.

Egom EE, Ke Y, Musa H, Mohamed TM, Wang T, Cartwright E, Solaro RJ and Lei M (2010) FTY720 prevents ischemia/reperfusion injury-associated arrhythmias in an ex vivo rat heart model via activation of Pak1/Akt signaling. *J Mol Cell Cardiol* **48**:406-414.

Esterbauer H, Schaur RJ and Zollner H (1991) Chemistry and biochemistry of 4-hydroxynonenal, malonaldehyde and related aldehydes. *Free Radic Biol Med* **11**:81-128.

Fishbein MC, Meerbaum S, Rit J, Lando U, Kanmatsuse K, Mercier JC, Corday E and Ganz W (1981) Early phase acute myocardial infarct size quantification: validation of the triphenyl tetrazolium chloride tissue enzyme staining technique. *Am Heart J* **101**:593-600.

Frangogiannis NG, Perrard JL, Mendoza LH, Burns AR, Lindsey ML, Ballantyne CM, Michael LH, Smith CW and Entman ML (1998) Stem cell factor induction is associated with mast cell accumulation after canine myocardial ischemia and reperfusion. *Circulation* **98**:687-698.

Gonzalez-Cabrera PJ, Jo E, Sanna MG, Brown S, Leaf N, Marsolais D, Schaeffer MT, Chapman J, Cameron M, Guerrero M, Roberts E and Rosen H (2008) Full pharmacological efficacy of a novel S1P1 agonist that does not require S1P-like headgroup interactions. *Mol Pharmacol* **74**:1308-1318.

Gray MO, Karliner JS and Mochly-Rosen D (1997) A selective epsilon-protein kinase C antagonist inhibits protection of cardiac myocytes from hypoxia-induced cell death. *J Biol Chem* **272**:30945-30951.

Greene LA and Tischler AS (1976) Establishment of a noradrenergic clonal line of rat adrenal pheochromocytoma cells which respond to nerve growth factor. *Proc Natl Acad Sci U S A* **73**:2424-2428.

Guo LP, Richardson KS, Tucker LM, Doll MA, Hein DW and Arteel GE (2004) Role of the renin-angiotensin system in hepatic ischemia reperfusion injury in rats. *Hepatology* **40**:583-589.

Inagaki K, Churchill E and Mochly-Rosen D (2006) Epsilon protein kinase C as a potential therapeutic target for the ischemic heart. *Cardiovasc Res* **70**:222-230.

Jin ZQ, Goetzl EJ and Karliner JS (2004) Sphingosine kinase activation mediates ischemic preconditioning in murine heart. *Circulation* **110**:1980-1989.

Jo E, Sanna MG, Gonzalez-Cabrera PJ, Thangada S, Tigyi G, Osborne DA, Hla T, Parrill AL and Rosen H (2005) S1P1-selective in vivo-active agonists from high-throughput screening: off-the-shelf chemical probes of receptor interactions, signaling, and fate. *Chem Biol* **12**:703-715.

Johnson JA, Gray MO, Chen CH and Mochly-Rosen D (1996) A protein kinase C translocation inhibitor as an isozyme-selective antagonist of cardiac function. *J Biol Chem* **271**:24962-24966.

Jolly PS, Bektas M, Olivera A, Gonzalez-Espinosa C, Proia RL, Rivera J, Milstien S and Spiegel S (2004) Transactivation of sphingosine-1-phosphate receptors by FcepsilonRI triggering is required for normal mast cell degranulation and chemotaxis. *J Exp Med* **199**:959-970.

Kaludercic N, Carpi A, Menabo R, Di Lisa F and Paolocci N (2011) Monoamine oxidases (MAO) in the pathogenesis of heart failure and ischemia/reperfusion injury. *Biochim Biophys Acta* **1813**:1323-1332.

Kaludercic N, Carpi A, Nagayama T, Sivakumaran V, Zhu G, Lai EW, Bedja D, De Mario A, Chen K, Gabrielson KL, Lindsey ML, Pacak K, Takimoto E, Shih JC, Kass DA, Di Lisa F and Paolocci N (2014) Monoamine oxidase B prompts mitochondrial and cardiac dysfunction in pressure overloaded hearts. *Antioxid Redox Signal* **20**:267-280.

Kaludercic N, Takimoto E, Nagayama T, Feng N, Lai EW, Bedja D, Chen K, Gabrielson KL, Blakely RD, Shih JC, Pacak K, Kass DA, Di Lisa F and Paolocci N (2010) Monoamine Oxidase A-Mediated Enhanced Catabolism of Norepinephrine

Contributes to Adverse Remodeling and Pump Failure in Hearts With Pressure Overload. *Circ Res* **106**:193-202.

Kaneko H, Koshi S, Hiraoka T, Miyauchi Y, Kitamura N and Inoue M (1998) Inhibition of post-ischemic reperfusion injury of the kidney by diamine oxidase. *Biochim Biophys Acta Mol Basis Dis* **1407**:193-199.

Keul P, van Borren MM, Ghanem A, Muller FU, Baartscheer A, Verkerk AO, Stumpel F, Schulte JS, Hamdani N, Linke WA, van LP, Matus M, Schmitz W, Stypmann J, Tiemann K, Ravesloot JH, Alewijnse AE, Hermann S, Spijkers LJ, Hiller KH, Herr D, Heusch G, Schafers M, Peters SL, Chun J and Levkau B (2016) Sphingosine-1-Phosphate Receptor 1 Regulates Cardiac Function by Modulating Ca2+ Sensitivity and Na+/H+ Exchange and Mediates Protection by Ischemic Preconditioning. *J Am Heart Assoc* **5**:e003393.

Koda K, Salazar-Rodriguez M, Corti F, Chan NY-K, Estephan R, Silver RB, Mochly-Rosen D and Levi R (2010) Aldehyde dehydrogenase activation prevents reperfusion arrhythmias by inhibiting local renin release from cardiac mast cells. *Circulation* **122**:771-781.

Kukreja RC (2012) PDE5 and Retargeting of Subcellular cGMP Signaling During Pathological Hypertrophy. *Circulation* **126**:916-919.

Levi R, Seyedi N, Schaefer U, Estephan R, Mackins CJ, Tyler E and Silver RB (2007) Histamine H_3-receptor signaling in cardiac sympathetic nerves: Identification of a novel MAPK-PLA_2-COX-PGE_2-EP_3R pathway. *Biochem Pharmacol* **73**:1146-1156.

Mackins CJ, Kano S, Seyedi N, Schafer U, Reid AC, Machida T, Silver RB and Levi R (2006) Cardiac mast cell-derived renin promotes local angiotensin formation,

norepinephrine release, and arrhythmias in ischemia/reperfusion. *J Clin Invest* **116**:1063-1070.

Means CK and Brown JH (2009) Sphingosine-1-phosphate receptor signalling in the heart. *Cardiovasc Res* **82**:193-200.

Mehta PK and Griendling KK (2007) Angiotensin II cell signaling: physiological and pathological effects in the cardiovascular system. *Am J Physiol Cell Physiol* **292**:C82-C97.

Nandagopal K, Dawson TM and Dawson VL (2001) Critical role for nitric oxide signaling in cardiac and neuronal ischemic preconditioning and tolerance. *J Pharmacol Exp Ther* **297**:474-478.

Obinata H and Hla T (2012) Sphingosine 1-phosphate in coagulation and inflammation. *Semin Immunopathol* **34**:73-91.

Oskeritzian CA, Alvarez SE, Hait NC, Price MM, Milstien S and Spiegel S (2008) Distinct roles of sphingosine kinases 1 and 2 in human mast-cell functions. *Blood* **111**:4193-4200.

Patella V, Marinò I, Arbustini E, Lamparter-Schummert B, Verga L, Adt M and Marone G (1998) Stem cell factor in mast cells and increased mast cell density in idiopathic and ischemic cardiomyopathy. *Circulation* **97**:971-978.

Redfors B, Shao Y and Omerovic E (2012) Myocardial infarct size and area at risk assessment in mice. *Exp Clin Cardiol* **17**:268-272.

Reid AC, Silver RB and Levi R (2007) Renin: at the heart of the mast cell. *Immunol Rev* **217**:123-140.

Safarian F, Khallaghi B, Ahmadiani A and Dargahi L (2015) Activation of S1P Receptor Regulates PI3K/Akt/FoxO3a Pathway in Response to Oxidative Stress in PC12 Cells. *J Mol Neurosci* **56**:177-187.

Selwyn AP and Braunwald E (2001) Ischemic Heart Disease, in *Harrison's Principles of Internal Medicine* (Braunwald E, Fauci AS, Kasper DL, Hauser SL, Longo DL and Jameson JL eds) pp 1399-1410, McGraw-Hill, New York.

Silver RB, Reid AC, Mackins CJ, Askwith T, Schaefer U, Herzlinger D and Levi R (2004) Mast cells: A unique source of renin. *Proc Natl Acad Sci U S A* **101**:13607-13612.

Takabe K, Paugh SW, Milstien S and Spiegel S (2008) "Inside-out" signaling of sphingosine-1-phosphate: therapeutic targets. *Pharmacol Rev* **60**:181-195.

Takai Y, Kishimoto A, Kikkawa U, Mori T and Nishizuka Y (1979) Unsaturated diacylglycerol as a possible messenger for the activation of calcium-activated, phospholipid-dependent protein kinase system. *Biochem Biophys Res Commun* **91**:1218-1224.

Tan AY and Verrier RL (2013) The role of the autonomic nervous system in cardiac arrhythmias. *Handb Clin Neurol* **117C**:135-145.

Veerappan A, Reid AC, Estephan R, O'Connor N, Thadani-Mulero M, Salazar-Rodriguez M, Levi R and Silver RB (2008) Mast cell renin and a local renin-angiotensin system in the airway: Role in bronchoconstriction. *Proc Natl Acad Sci U S A* **105**:1315-1320.

Vessey DA, Li L, Honbo N and Karliner JS (2009) Sphingosine 1-Phosphate is an Important Endogenous Cardioprotectant Released by Ischemic Pre- and Post-Conditioning. *Am J Physiol Heart Circ Physiol* **297**:H1429-H1435.

Vitalis T, Alvarez C, Chen K, Shih JC, Gaspar P and Cases O (2003) Developmental expression pattern of monoamine oxidases in sensory organs and neural crest derivatives. *J Comp Neurol* **464**:392-403.

Walker MJA, Curtis MJ, Hearse DJ, Campbell RW, Janse MJ, Yellon DM, Cobbe SM, Coker SJ, Harness JB, Harron DW, Higgins AJ, Julian DG, Lab MJ, Manning AS, Northover BJ, Parratt JR, Riemersma RA, Riva E, Russell DC, Sheridan DJ, Winslow E and Woodward B (1988) The Lambeth Conventions: guidelines for the study of arrhythmias in ischaemia, infarction, and reperfusion. *Cardiovasc Res* **22**:447-455.

Wen H, Gwathmey JK and Xie LH (2012) Oxidative stress-mediated effects of angiotensin II in the cardiovascular system. *World J Hypertens* **2**:34-44.

Xiao Q, Weiner H and Crabb DW (1996) The mutation in the mitochondrial aldehyde dehydrogenase (ALDH2) gene responsible for alcohol-induced flushing increases turnover of the enzyme tetramers in a dominant fashion. *J Clin Invest* **98**:2027-2032.

Yung BS, Brand CS, Xiang SY, Gray CB, Means CK, Rosen H, Chun J, Purcell N, Brown JH and Miyamoto S (2017) Selective coupling of the S1P3 receptor subtype to S1P-mediated RhoA activation and cardioprotection. *J Mol Cell Cardiol* **103**:1-10.

Zambelli VO, Gross ER, Chen CH, Gutierrez VP, Cury Y and Mochly-Rosen D (2014) Aldehyde dehydrogenase-2 regulates nociception in rodent models of acute inflammatory pain. *Sci Transl Med* **6**:251ra118.

Footnote

This research was supported by the National Institutes of Health [Grant HL034215] and the American Heart Association [Grant-in-Aid]

JPET Fast Forward. Published on May 12, 2017 as DOI: 10.1124/jpet.117.241976
This article has not been copyedited and formatted. The final version may differ from this version.

Figure Legends

Figure 1. $S1P_1R$ activation provides anti-RAS IPC-like cardioprotection in an isolated guinea-pig heart model of I/R. $S1P_1R$ blockade, PKCε inhibition and ALDH2 inactivation prevent IPC-like cardioprotection.

All guinea pig hearts were subjected to 20-min global ischemia followed by 30-min reperfusion either in the absence (Control, *n* = 8) or the presence of W146 ($S1P_1R$ antagonist, 1 μM; *n* = 15) and SEW2871 ($S1P_1R$ agonist, 1 μM; *n* = 10). When necessary, W146 ($S1P_1R$ antagonist, 1 μM; *n* = 15), $\varepsilon V_{1\text{-}2}$ (PKCε inhibitor, 1 μM; *n* = 8), or GTN (ALDH2 inactivator, 2 μM; *n* = 8) were added in the presence of SEW2871 ($S1P_1R$ agonist, 1 μM). Other hearts were subjected to I/R preceded by IPC alone (i.e., 2 x 5-min cycles of ischemia, each followed by 5-min reperfusion, n = 14) or in the presence of W146 (1 μM; *n* = 8). Bars indicate means ± SEM of independent experiments. (**A**) Duration of reperfusion arrhythmias (VT/VF). (**B**) Overflow of NE and (**C**) Ang I-forming activity collected over 6 min either before ischemia or at the start of reperfusion. *, P < 0.05; **, P < 0.01; ***, P < 0.001, by unpaired *t*-test. **D-F**: Representative ECG recordings from guinea pig hearts before ischemia (Control, **D**), at the start of reperfusion (**E**) and at the end of VT/VF (Recovery, **F**).

Figure 2. $S1P_1R$ activation affords anti-RAS IPC-like cardioprotection in a WT isolated murine heart model of I/R, but not in ALDH2*2 hearts.

Mouse hearts were subjected to 40-min global ischemia followed by 30-min reperfusion (Control, WT, *n* = 9; ALDH2*2, *n* = 9). Other hearts were subjected I/R preceded by IPC alone (WT, *n* = 8; ALDH2*2, *n* = 15) or in the presence of W146 (3 μM; WT, *n* = 9). Other hearts were perfused with SEW2871 alone (0.1 μM; WT, *n* =

JPET Fast Forward. Published on May 12, 2017 as DOI: 10.1124/jpet.117.241976
This article has not been copyedited and formatted. The final version may differ from this version.

13; ALDH2*2, *n* = 14) or in the presence of W146 (3 μM; WT, *n* = 8; ALDH2*2, *n* = 6), $\varepsilon V_{1\text{-}2}$ (1 μM; WT, *n* = 6; ALDH2*2, *n* = 6), or GTN (2 μM; WT, *n* = 6; ALDH2*2, *n* = 6). (**A**) Duration of reperfusion arrhythmias (VT/VF). Overflow of NE (**B**) and Ang I-forming activity (**C**) collected over 2 min before ischemia and 6 min at the start of reperfusion. Bars indicate means ± SEM of independent experiments. *, P < 0.05; **, P < 0.01; ***, P < 0.001, by unpaired *t*-test. **D-F**: Representative ECG recordings from mouse hearts before ischemia (Control, **D**), at the start of reperfusion (**E**) and at the end of VT/VF (Recovery, **F**).

Figure. 3. $S1P_1R$ activation reduces the area of I/R-induced ischemic injury in WT, but not in ALDH2*2 hearts.

(**A**) Qualitative and (**B**) quantitative representation of TTC staining in 2-mm-thick left ventricle slices. WT and ALDH2*2 mouse hearts were subjected to 120-min reperfusion (I/R, WT, *n* = 5; ALDH2*2, *n* = 7), with SEW2871 alone (0.1 μM WT, *n* = 6; ALDH2*2, *n* = 6) or in the presence of W146 (3 μM; WT, *n* = 6; ALDH2*2, *n* = 6). Other hearts were analyzed after IPC (WT, *n* = 5; ALDH2*2, *n* = 8). Scale bar in panel A is 1 mm. Bars indicate means ± SEM of independent experiments. Pale areas indicate I/R-injured tissue, while healthy tissue is colored in red. *, P < 0.05; **, P < 0.01; ***, P < 0.001, by unpaired *t*-test.

Figure 4. $S1P_1R$ is expressed in HMC-1, BMMC WT and BMMC ALDH2*2 and its activation enhances PKCε translocation.

(**A**) Representative Western blot of total lysate of HMC-1, BMMC WT and BMMC ALDH2*2 (50 μg protein/lane) and Jurkat cells (positive control, 15 μg protein/lane) probed with anti-$S1P_1R$ antibody. (**B**) Double immunofluorescence staining of $S1P_1R$

JPET Fast Forward. Published on May 12, 2017 as DOI: 10.1124/jpet.117.241976
This article has not been copyedited and formatted. The final version may differ from this version.

(green) and c-Kit (red) in WT- and ALDH2*2-BMMC. (**C**-**E**) PKCε translocation in (**C**) HMC-1, (**D**) WT-BMMC and (**E**) ALDH2*2-BMMC. Incubation of HMC-1, BMMC WT and ALDH2*2 with $S1P_1R$ agonist (SEW2871, 1 μM and 0.1 μM, respectively, 10 min) and PMA (10 nM, min, positive control) enhances PKCε translocation from cytosol to membrane in all three cells lines. Bars represent the quantification of PKCε translocated from the cytosol to membrane fraction normalized over β-actin and are means ± SEM (Control, *n* = 7, 8, 6; PMA, *n* = 9, 7, 5; SEW2871, *n* = 10, 5, 5; SEW2871+W146, *n* = 5, 4, 6 in HMC-1, WT-BMMC, ALDH2*2-BMMC, respectively). *, P < 0.05; **, P < 0.01, ***, P < 0.001, by unpaired *t*-test.

Figure 5. Activation of $S1P_1R$ enhances ALDH2 activity in HMC-1 and WT-BMMC but not in ALDH2*2-BMMC

Incubation with the ALDH2 activator Alda-1 (300 μM, 10 min, positive control), PMA (300 or 10 nM, 10 min), or SEW2871 (1 μM or 0.1 μM, 10 min) enhances ALDH2 activity in (**A**) HMC-1 and (**B**) WT-BMMC but not in (**C**) ALDH2*2- BMMC. Pretreatment with W146 (1 or 0.1 μM, 20 min), εV_{1-2} (1 μM, 20 min), or GTN (2 μM, 30 min) prevents the effects of the $S1P_1R$ agonist in HMC-1 (**A**) and WT-BMMC (**B**) but not in ALDH2*2- BMMC (**C**). Bars are means ± SEM of percent increases from control (HMC-1, WT-BMMC, ALDH2*2-BMMC, respectively: control, *n* = 12, 17, 17; PMA, *n* = 9, 8, 7; Alda-1, *n* = 10, 8, 6; SEW2871, *n* = 17, 9, 7; SEW2871+W146, *n* = 5, 8, 6; SEW2871+εV_{1-2}, *n* = 5, 5, 6; SEW2871+GTN, *n* = 7, 4, 4). Basal NADH production was 3.5 ± 0.21 μmol/min/mg protein in HMC-1, 0.96 ± 0.12 μmol/min/mg protein in WT-BMMC, 0.63 ± 0.11 μmol/min/mg protein in ALDH2*2-BMMC. *, P < 0.05; **, P < 0.01; ***, P < 0.001 vs. control, by one-way ANOVA followed by Dunnett's post hoc test.

JPET Fast Forward. Published on May 12, 2017 as DOI: 10.1124/jpet.117.241976
This article has not been copyedited and formatted. The final version may differ from this version.

Figure 6. Alda-1 increase ALDH2 activity and reduces acetaldehyde-induced degranulation and renin release in WT-BMMC but not in ALDH2*2-BMMC cells.

(**A**) Incubation of WT-BMMC and ALDH2*2-BMMC with the selective ALDH2 activator Alda-1 (300 μM, 10 min) elicits an increase in ALDH2 activity in WT-BMMC (*n* = 7) but not in ALDH2*2-BMMC cells (*n* = 5). Basal NADH production was 0.96 ± 0.12 μmol/min/mg protein in WT-BMMC (*n* = 17), 0.63 ± 0.11 μmol/min/mg protein in ALDH2*2-BMMC (*n* = 17). (**B**) Enzymatic activity of ALDH2 in WT-BMMC and ALDH2*2-BMMC cells. Curves start at 5 min, time at which the activity began in all samples. (**C** and **D**) Incubation with acetaldehyde (100 μM, 20 min, 37°C) induces release of β-HEX and renin release in WT-BMMC (*n* = 20 and 12, respectively) and ALDH2*2-BMMC cells (*n* = 20 and 8, respectively). Preincubation with Alda-1 (20 μM, 10 min, 37°C) inhibits degranulation and renin release in WT-BMMC (*n* = 6 and 5, respectively) but not in ADH2*2- BMMC (*n* = 9 and 5, respectively). Bars are means ± SEM. β-HEX and renin were measured in the supernatants at the end of acetaldehyde incubation. * P<0.05; **, P<0.01, ***P<0.001 by unpaired *t*-test.

Figure 7. $S1P_1R$ activation attenuates acetaldehyde-induced degranulation and renin release in HMC-1 and WT-BMMC but not in ALDH2*2-BMMC.

Incubation with SEW2871 (0.1 and 1 μM, 10 min) diminishes degranulation and renin release evoked by acetaldehyde (100-300 μM, 20 min) in (**A**) HMC-1, (**B**) WT-BMMC but not in (**C**) ALDH2*2 cells. Pretreatment with W146 (0.1 and 1 μM, 20 min), εV_{1-2} (1 μM, 20 min), or GTN (2 μM, 30 min) prevent the effect of the $S1P_1R$ agonist in (**A**) HMC-1, (**B**) WT-BMMC and (**C**) ALDH2*2-BMMC cells. Bars are means ± SEM of percent increases above control (β-HEX and renin in HMC-1, WT-BMMC, ALDH2*2-BMMC, respectively: acetaldehyde, *n* = 20, 22, 19 and *n* = 9, 13, 8; SEW2871, *n* = 9,

JPET Fast Forward. Published on May 12, 2017 as DOI: 10.1124/jpet.117.241976
This article has not been copyedited and formatted. The final version may differ from this version.

10, 7 and 9, 10, 7; SEW2871+W146, *n* = 17, 14, 13 and *n* = 7, 10, 6; SEW2871+εV$_{1-2}$, *n* = 5, 5, 5 and *n* = 5, 5, 5; SEW2871+GTN, *n* = 7, 5, 5 and *n* = 5, 5, 5). β-HEX and renin content was measured in the supernatants at the end of acetaldehyde incubation. Basal β-HEX in HMC-1, WT-BMMC and ALDH2*2-BMMC was 3.14 ± 0.41 (n = 14), 2.87 ± 0.27 (n = 23) and 2.92 ± 0.31 (n = 21) % of total, respectively; basal renin release (Ang-I formed) for HMC-1 was 18.26 ± 4.12 (n = 17) ng/hr/mg protein and for WT-BMMC and ALDH2*2-BMMC was 0.25 ± 0.04 (n = 29) and 0.49 ± 0.15 (n = 22) μg/hr/mg protein, respectively. *, P<0.05; **, P<0.01, ***, P<0.001 by unpaired *t*-test.

Figure 8. S1P$_1$R activation attenuates 4-HNE induced degranulation and renin release in HMC-1 and WT-BMMC but not in ALDH2*2-BMMC.

Incubation with SEW2871 (0.1 and 1 μM, 10 min) diminishes degranulation (i.e., β-HEX) and renin release evoked by 4-HNE (30 μM, 20 min) in (**A**) HMC-1, (**B**) WT-BMMC but not in (**C**) ALDH2*2 cells. Pretreatment with W146 (0.1 and 1 μM, 20 min) prevents the effect of the S1P$_1$R agonist in (**A**) HMC-1, (**B**) WT-BMMC and (**C**) ALDH2*2-BMMC cells. Bars are means ± SEM of percent increases above control (β-HEX and renin in HMC-1, WT-BMMC, ALDH2*2-BMMC, respectively: 4-HNE, *n* = 5, 7, 7 and *n* = 5, 5, 5; SEW2871, *n* = 5, 6, 5 and 5, 5, 5; SEW2871+W146, *n* = 5, 6, 5 and 5, 5, 5). β-HEX and renin content was measured in the supernatants at the end of 4-HNE incubation. Basal β-HEX in HMC-1, WT-BMMC and ALDH2*2-BMMC was 4.61 ± 0.17 (n = 5), 3.08 ± 0.58 (n = 7) and 2.17 ± 0.25 (n = 7) % of total, respectively; basal renin release (Ang-I formed) for HMC-1 was 5.25 ± 0.42 (n = 6) ng/hr/mg protein and

JPET Fast Forward. Published on May 12, 2017 as DOI: 10.1124/jpet.117.241976
This article has not been copyedited and formatted. The final version may differ from this version.

for WT-BMMC and ALDH2*2-BMMC was 0.36 ± 0.12 (n = 6) and 0.20 ± 0.08 (n = 5) μg/hr/mg protein, respectively. *, P<0.05; **, P<0.01, ***, P<0.001 by unpaired *t*-test

Figure 9. Schematic representation of our findings, and the pathway downstream of S1P$_1$R activation as a novel anti-RAS cardioprotective mechanism.

JPET Fast Forward. Published on May 12, 2017 as DOI: 10.1124/jpet.117.241976
This article has not been copyedited and formatted. The final version may differ from this version.

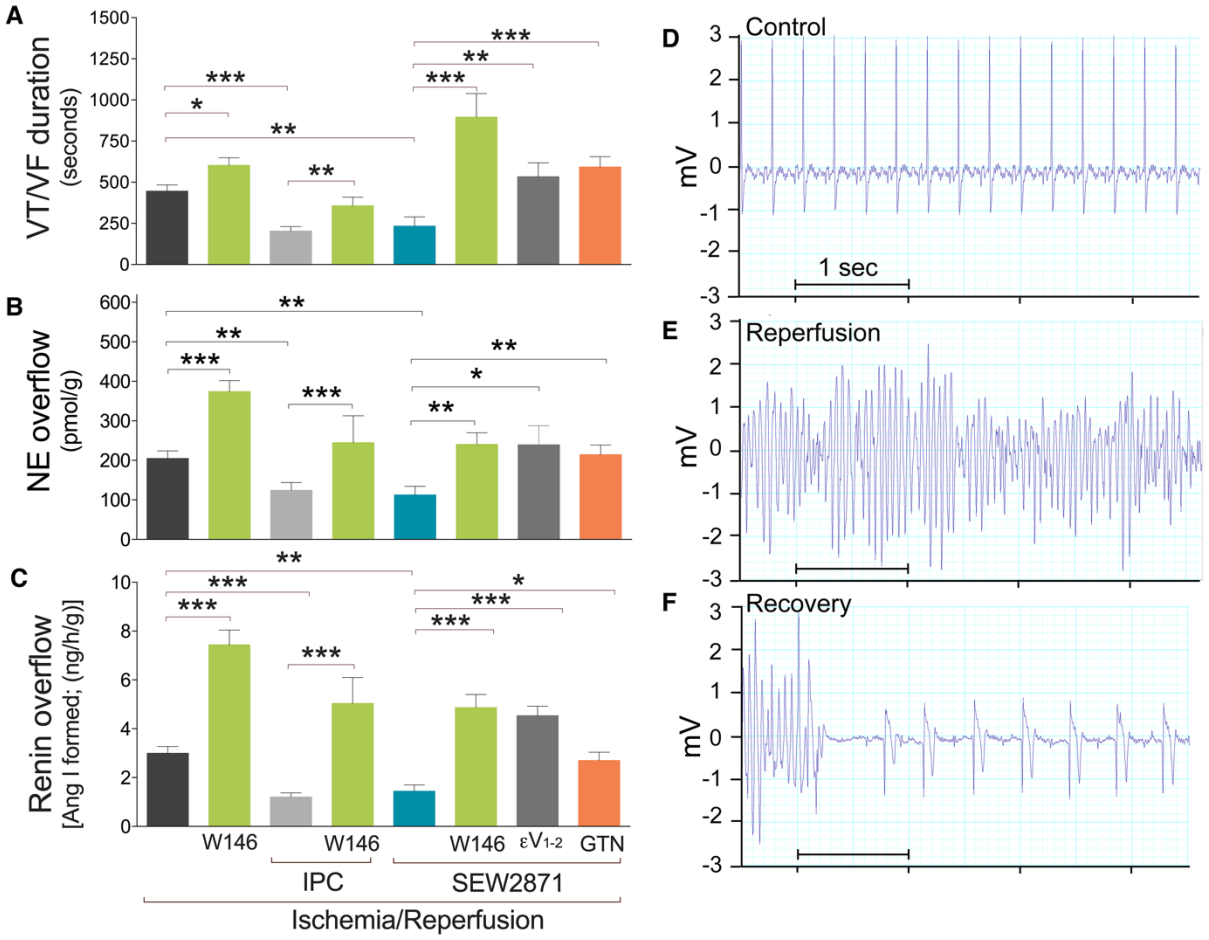

Fig.1

JPET Fast Forward. Published on May 12, 2017 as DOI: 10.1124/jpet.117.241976
This article has not been copyedited and formatted. The final version may differ from this version.

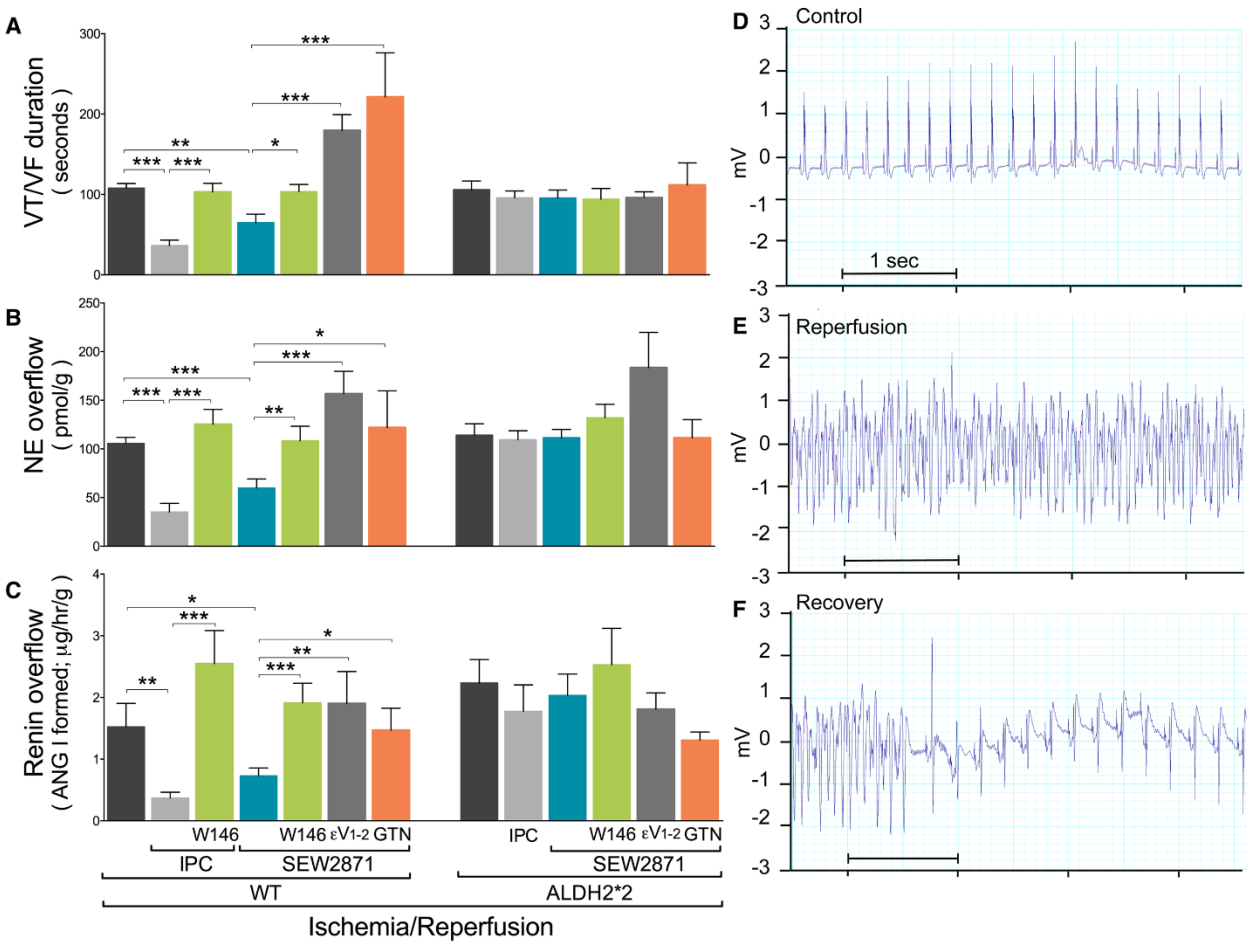

Fig.2

JPET Fast Forward. Published on May 12, 2017 as DOI: 10.1124/jpet.117.241976
This article has not been copyedited and formatted. The final version may differ from this version.

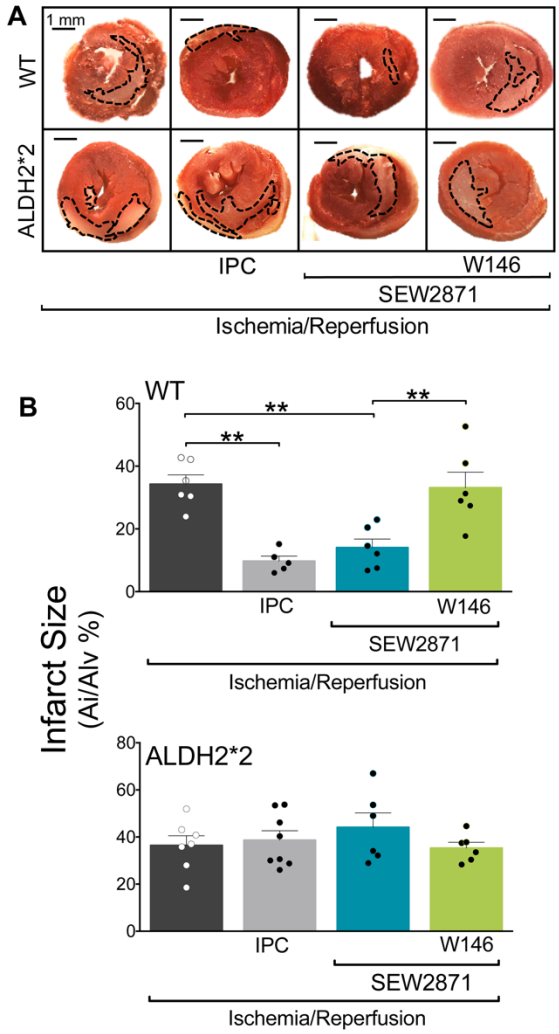

Fig.3

JPET Fast Forward. Published on May 12, 2017 as DOI: 10.1124/jpet.117.241976
This article has not been copyedited and formatted. The final version may differ from this version.

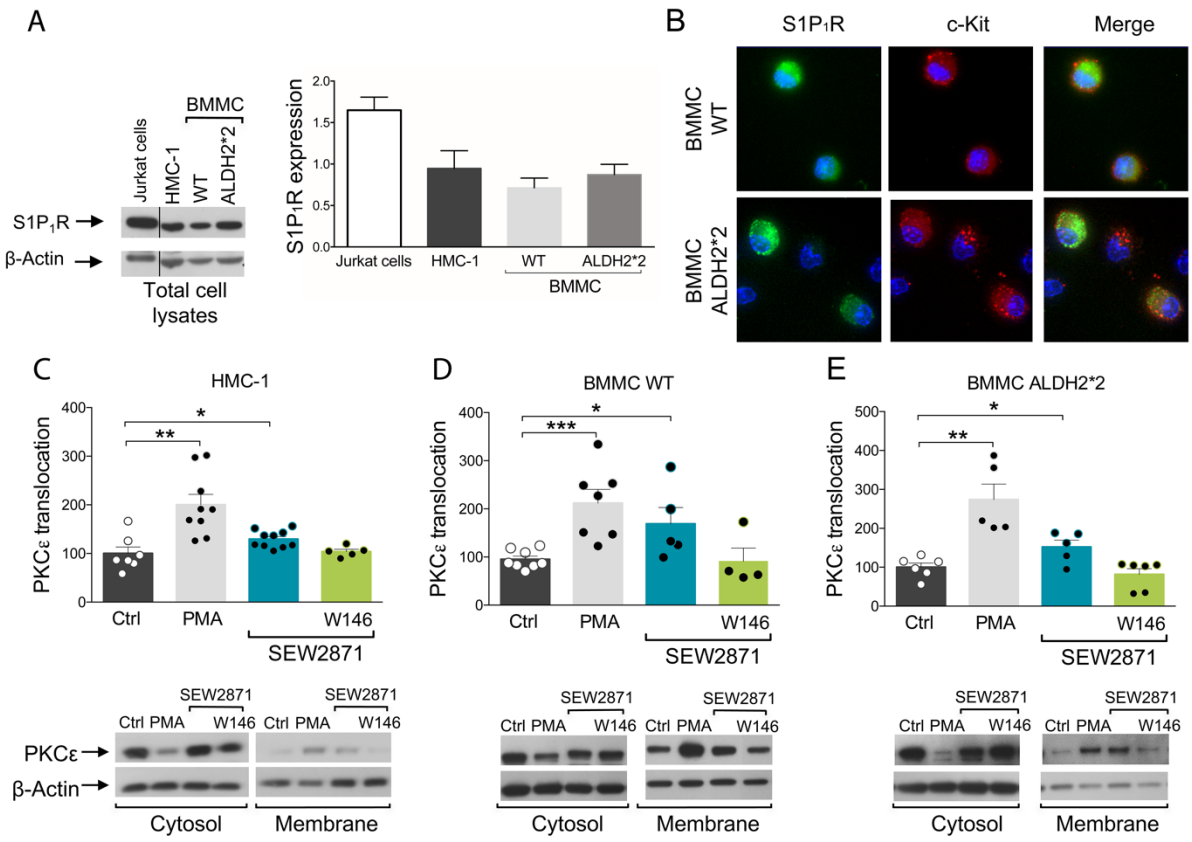

Fig.4

JPET Fast Forward. Published on May 12, 2017 as DOI: 10.1124/jpet.117.241976
This article has not been copyedited and formatted. The final version may differ from this version.

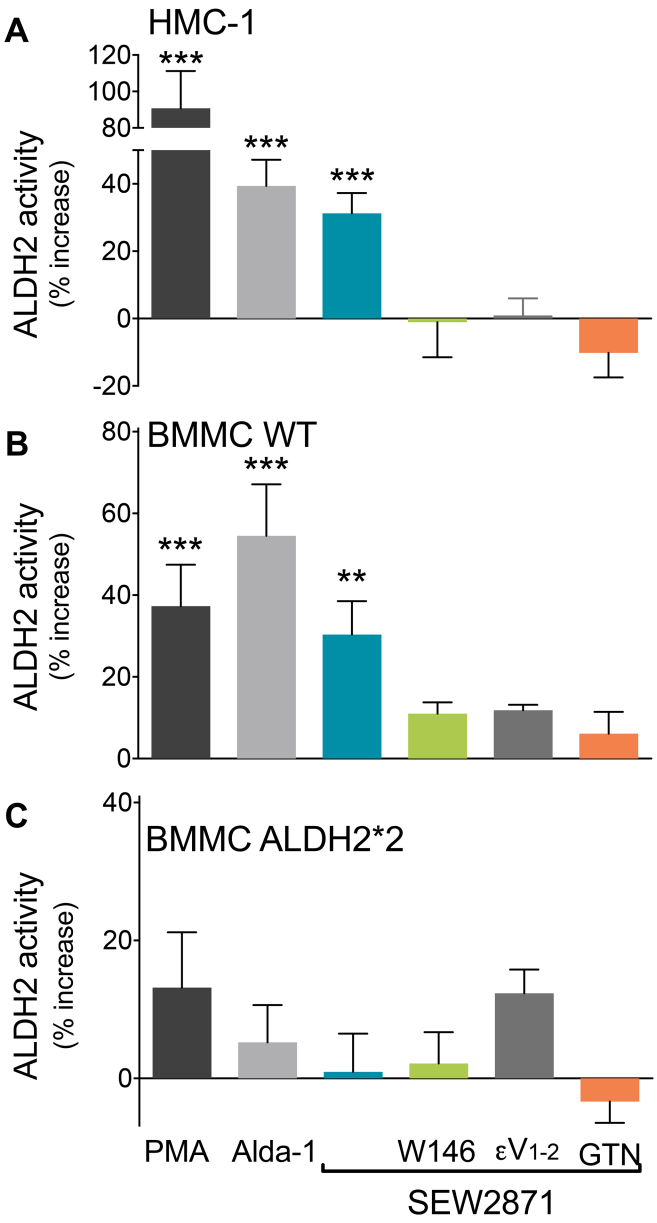

Fig.5

JPET Fast Forward. Published on May 12, 2017 as DOI: 10.1124/jpet.117.241976
This article has not been copyedited and formatted. The final version may differ from this version.

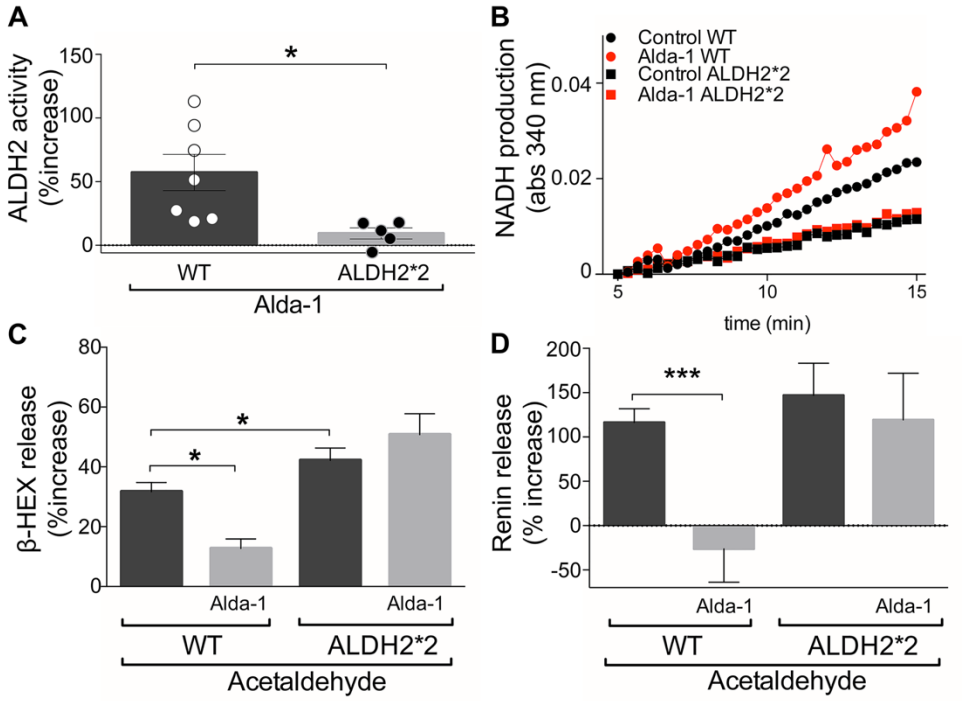

Fig.6

JPET Fast Forward. Published on May 12, 2017 as DOI: 10.1124/jpet.117.241976
This article has not been copyedited and formatted. The final version may differ from this version.

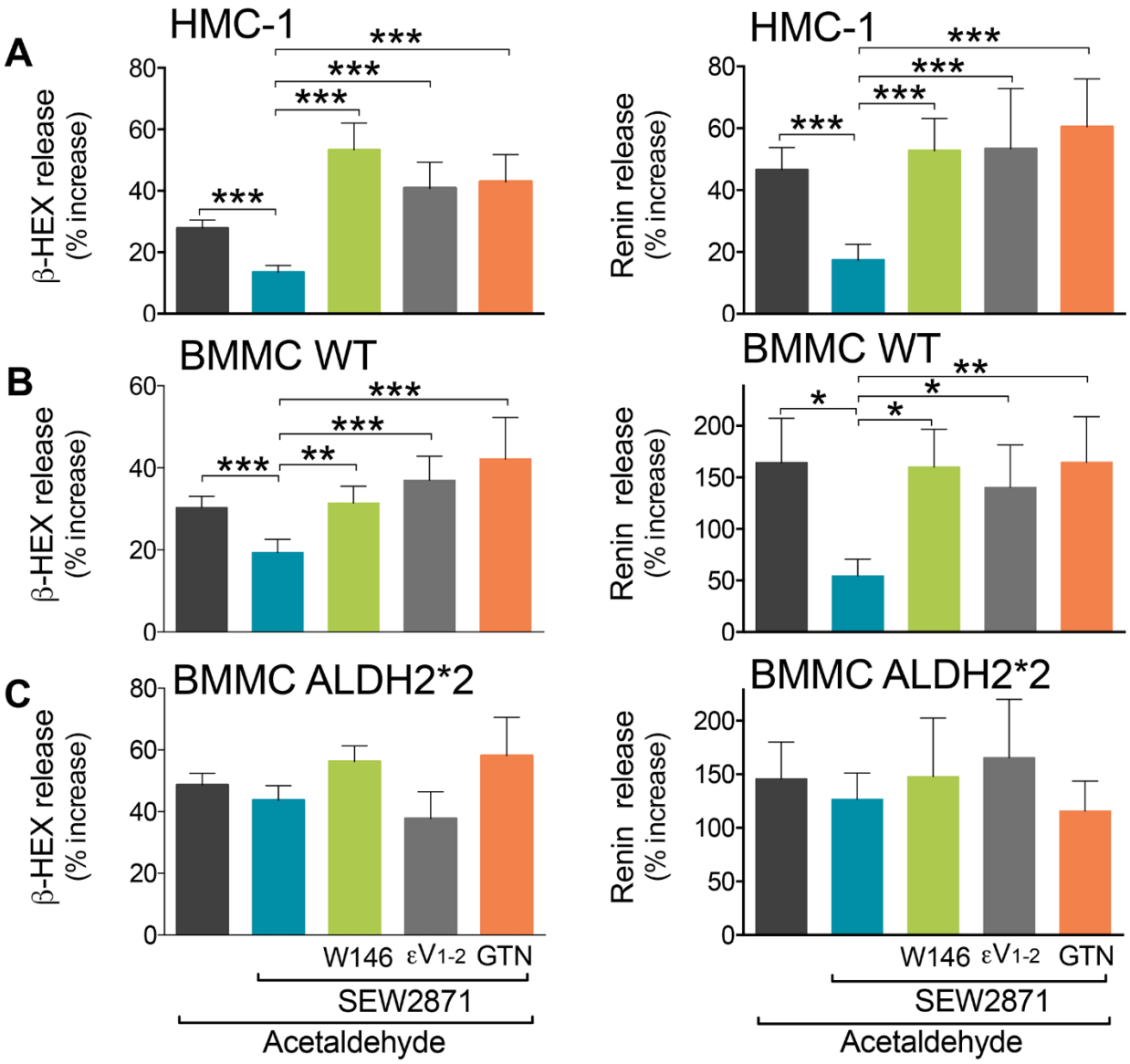

Fig.7

JPET Fast Forward. Published on May 12, 2017 as DOI: 10.1124/jpet.117.241976
This article has not been copyedited and formatted. The final version may differ from this version.

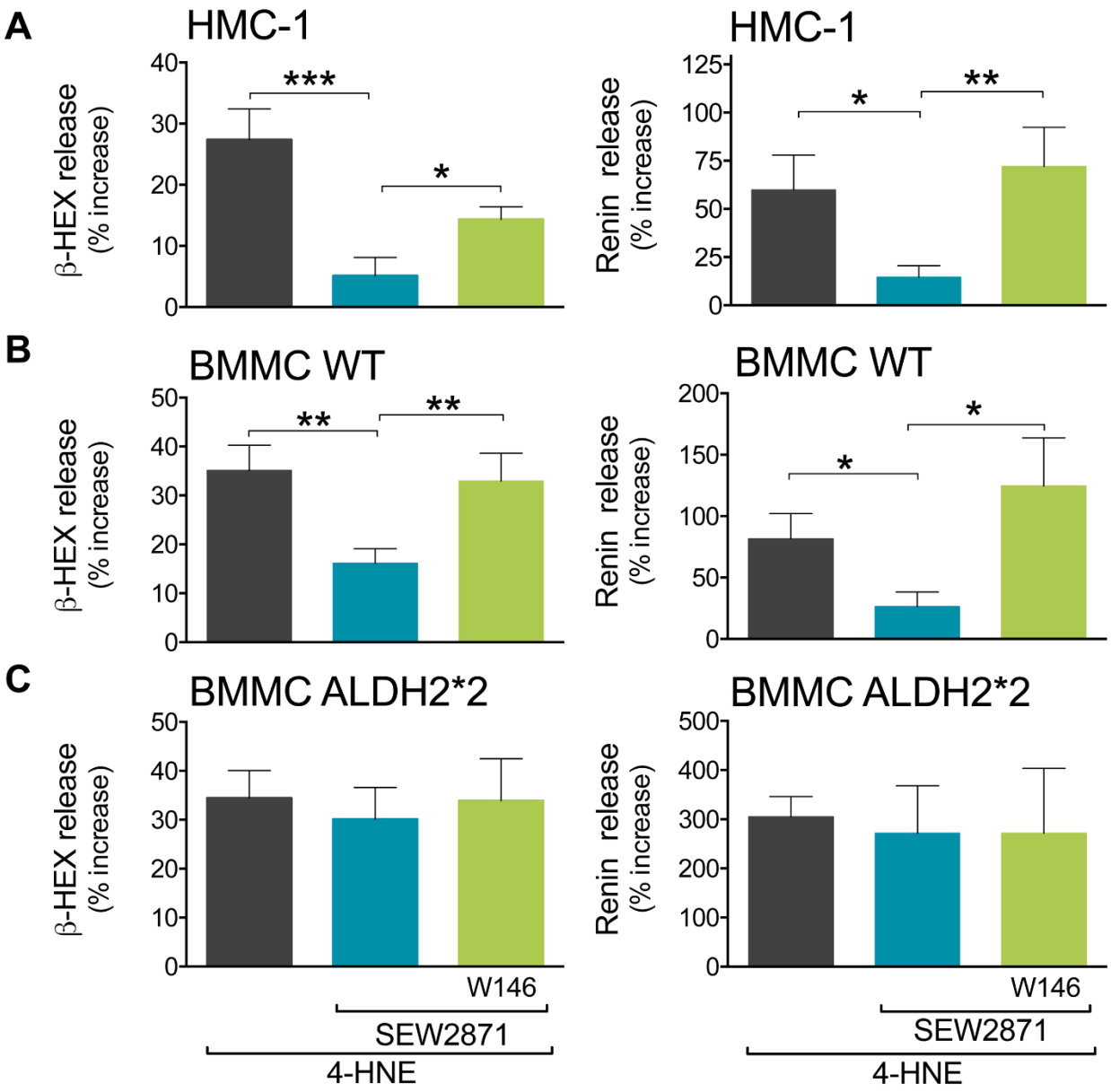

Fig.8

JPET Fast Forward. Published on May 12, 2017 as DOI: 10.1124/jpet.117.241976
This article has not been copyedited and formatted. The final version may differ from this version.

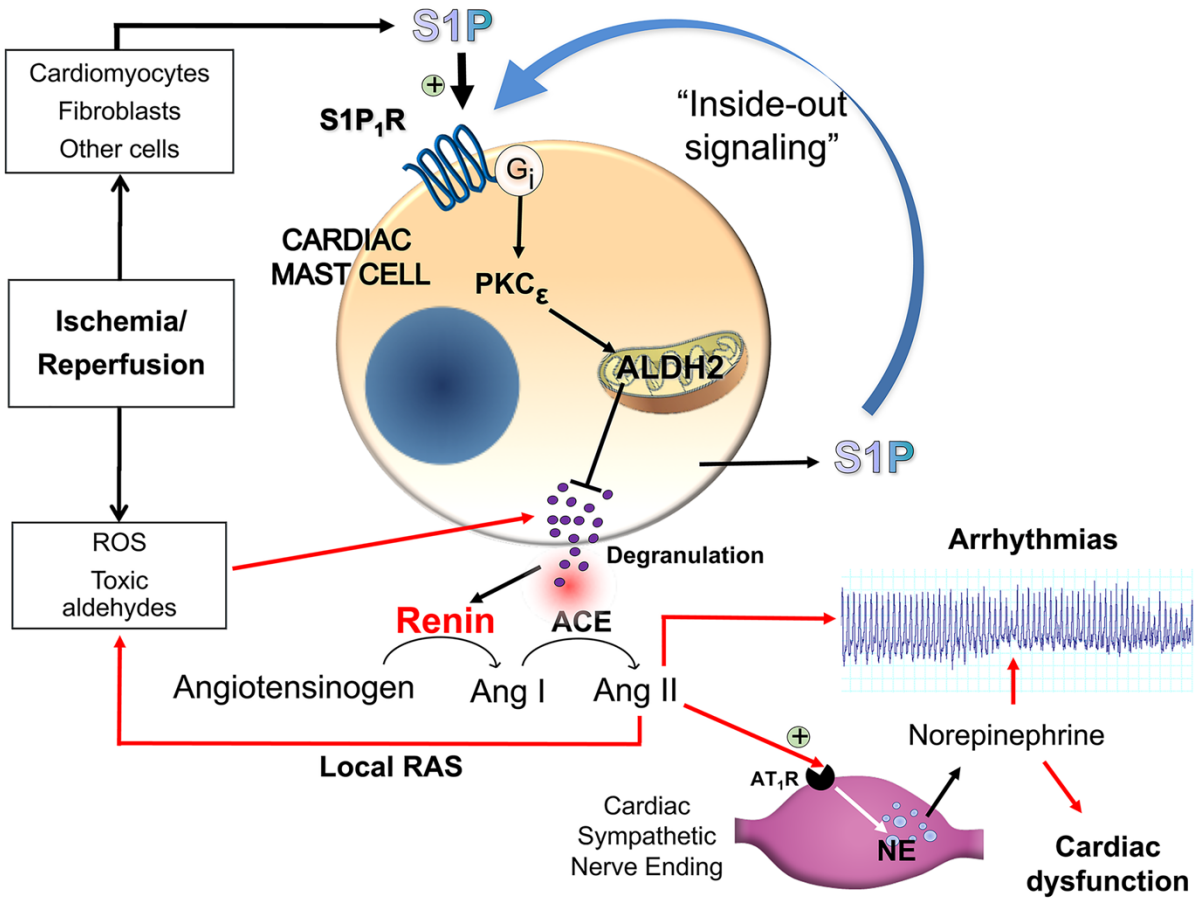

Fig.9